Mechanisms of action of Ru(ii) polypyridyl complexes in living cells upon light irradiation

Jakubaszek, Marta ; Goud, Bruno ; Ferrari, Stefano ; Gasser, Gilles

Abstract: The unique photophysical properties of Ru(ii) polypyridyl complexes make them very attractive candidates as photosensitisers in Photodynamic Therapy (PDT). However, to date, there are not many studies exploring in detail the mechanism(s) of action of such compounds in living systems upon light irradiation. This feature article provides an overview of the most in-depth biological studies on such compounds.

DOI: https://doi.org/10.1039/c8cc05928d

Mechanisms of Action of Ru(II) Polypyridyl Complexes in Living Cells upon Light Irradiation

*Marta Jakubaszek,[a,b] Bruno Goud,[b] Stefano Ferrari,[c] and Gilles Gasser[a,]**

[a] Chimie ParisTech, PSL University, Laboratory for Inorganic Chemical Biology, Paris, France.

[b] Institut Curie, PSL University, CNRS UMR 144, Paris, France

[c] Institute of Molecular Cancer Research, University of Zurich, Zurich, Switzerland.

* Email: gilles.gasser@chimieparistech.psl.eu; www.gassergroup.com; Tel. +33 1 44 27 56 02.

ORCID-ID:

Marta Jakubaszek: 0000-0001-7590-2330

Bruno Goud: 0000-0003-1227-4159

Stefano Ferrari: 0000-0002-6607-215X

Gilles Gasser: 0000-0002-4244-5097

Abstract

The unique photophysical properties of Ru(II) polypyridyl complexes make them very attractive candidates as photosensitisers in Photodynamic Therapy (PDT). However, to date, there are not many studies exploring in detail the mechanism(s) of action of such compounds in living systems upon light irradiation. This feature article provides an overview of the most in-depth biological studies on such compounds.

Introduction

The earliest reports on the use of light in combination with chemical entities in the field of medicine are more than 100 years old.[1] Since then, this medical technique, known as photodynamic therapy (PDT), has evolved to a successful alternative or complimentary treatment to chemotherapy, radiotherapy and surgery. Nowadays PDT is an approved and common treatment in dermatology. It is used to treat acne, psoriasis, keloid scars and port wine stains, helping patients to improve their appearance and quality of life.[2, 3] PDT also gives another, new perspective for cancer therapy due to its spatial and temporal control.[4] This treatment modality is currently approved for a wide range of cancer types using commercially available photosensitisers such as Photofrin®, Visudyne®, Foscan® or Levulan® (see Figure 1 for structures).[5, 6]

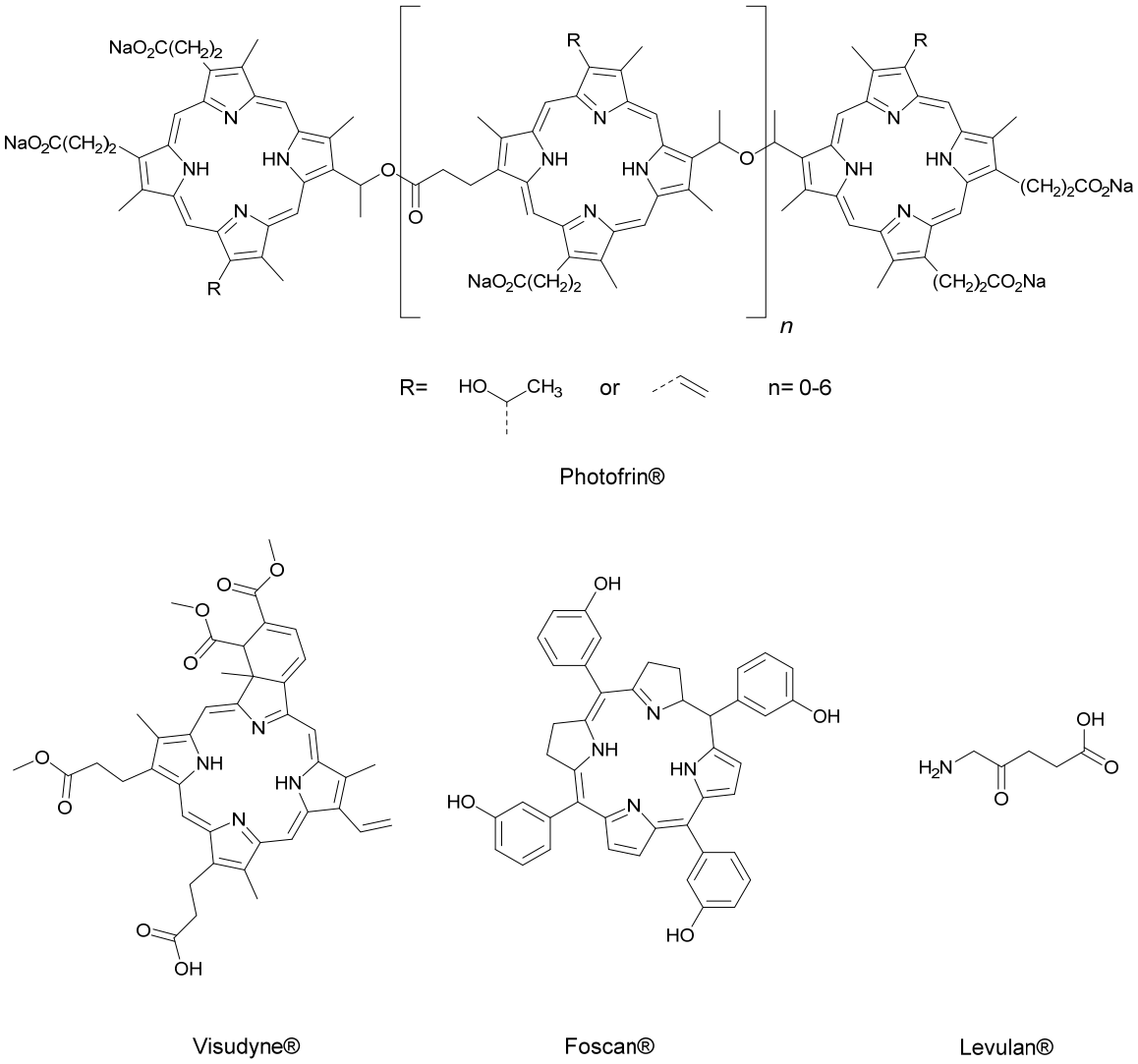

Figure 1. Chemical structures of Photofrin®, Visudyne®, Foscan® and Levulan®.

PDT usually requires three main components, namely a photosensitiser (PS), molecular oxygen ($^3O_2$) and light. After injection/application of the PS into/on the patient, the latter is irradiated at a specific, defined wavelength, allowing the PS to reach its singlet excited state $^1PS^*$. After intersystem crossing (ISC), the PS reaches an excited state, which has a triplet character ($^3PS^*$). It might then react in two different electron exchange mechanisms, resulting in the formation of very reactive singlet oxygen $^1O_2$ (Type II) or radical anions or cations, which can further react with oxygen producing other reactive oxygen species (ROS) like hydrogen peroxide H_2O_2, superoxide O_2^- or hydroxyl radicals $^{\bullet}OH$ (Type I). Both mechanisms, namely Types I and II, lead to the formation of products that impair metabolic pathways and eventually lead to

eukaryotic cell or bacteria death. The ratio between these two processes depends on the PS used as well as the concentrations of molecular oxygen and other biological substrates.[7] The most attractive feature of PDT is its subsistent selectivity. Indeed, areas that are affected by PDT treatments are only those where the PS has accumulated and where light is applied. Additionally, due to the short life of generated $^1O_2$ (40 ns) and radicals, the area of action is estimated to be only 20 nm.[8]

Currently used PSs are based on cyclic tetrapyrrolic structures like porphyrins, phtalocyanines or chlorins.[9] Although they fill the requirements of a PS, they also have a number of drawbacks. Photofrin®, for example, exhibits poor light penetration into the tumour as well as low clearance from the patients bodies that leads to photosensitivity.[10] There is therefore a need for new PSs that overcome these unwanted effects and that have a higher uptake and selectivity towards cancer cells.[11] Recently designed molecules can be classified in two main classes, namely modified porphyrin-based PSs or porphyrin-free PDT systems.[6] In the second class, inert Ru(II) polypyridyl complexes have raised great interest not only as alternatives to cisplatin but also as a novel PDT PSs because of their favourable photophysical properties (e.g. long excited state lifetimes, visible light absorption and two-photon excitation).[6, 12-15] One of these compounds, namely TLD-1433, is currently undergoing a human clinical trial against invasive bladder cancer (Figure 2).

Understanding the mechanism(s) of action of these compounds in living cells/mice upon light irradiation is extremely important to establish their therapeutic potential and to design new generation PSs. Unfortunately, to date, there is a scarcity of studies exploring in depth the mode(s) of action of these compounds.[16] In this feature article, we review only biological studies that describe more than just the phototoxicity and the cellular localisation of some Ru(II) complexes, starting from the results obtained with TLD-1433, the PS of the McFarland group currently in clinical trial. To the end of our feature article, we have decided to classify the Ru(II)

complexes depending on their cellular localisation. Of note, only coordinatively saturated and substitutionally inert Ru(II) polypyridyl complexes are discussed herein.

TLD-1433 and its derivatives

In 2013, the group of prof. McFarland reported two compounds, namely **TLD-1411** and **TLD-1433** (see Figure 2).[17] Both molecules were first investigated for photodynamic inactivation (PDI) of pathogenic bacteria.

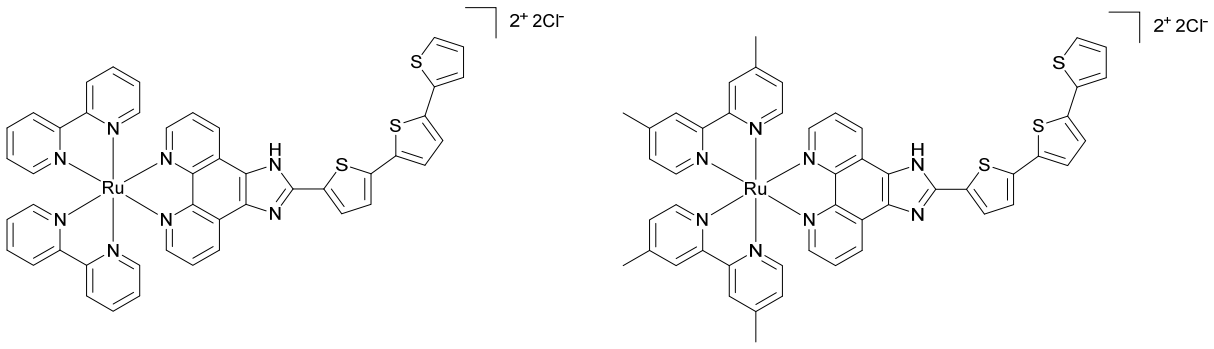

Figure 2. TLD-1411 and TLD-1433

The researchers pointed out that the 2-(2',2'':5'',2'''-terthiophene)-imidazo[4,5-f][1,10]phenanthroline (IP-TT) ligand in the compounds structure might be responsible for both Type I and Type II electron exchange mechanisms. The ability of the designed complexes to work in low oxygen conditions through a Type I mechanism corroborated the advantage of these compounds. Promising results obtained in bacteria led to further examinations of the compounds. In 2015, a study on **TLD-1411** and **TLD-1433** as PSs suitable for anticancer PDT *in vitro* and *in viv*o was reported by Lilge and co-workers.[18] For *in vitro* studies, four cell lines were used, namely CT26 and CT25.26 (respectively wild type and N-nitroso-N-methylurethane-induced mouse colon carcinoma), U87MG (human glioblastoma cell line) and F98 (rat glioblastoma). The Lethal Dose to kill 50 % of the cell population (LD_{50}) was determined for **TLD-1411** and **TLD-1433** on all four cell lines in the dark and after light irradiation. Concentration of 4 μM of **TLD-1411** and 1 μM of **TLD-1433** effectively killed 100% of CT-26 WT and U87MG cells upon light irradiation (green LED emitting at 525 ± 25

nm; 45 J cm^{-2}). U87MG cells were chosen to check whether these PSs could be used in hypoxic and normoxic conditions. A photodynamic effect was observed in normoxic conditions with concentrations of 18 μM (70% of cells killed). Unfortunately, **TLD-1411** and **TLD-1433** did not work in hypoxia conditions in human cell lines. The compounds were also tested *in vivo* using 8-10 week-old BALB/C mice injected with CT26.WT murine colon carcinoma. The maximum tolerated dose 50 (MTD_{50}) values for **TLD-1411** and **TLD-1433** were established to be 36 $mg{\cdot}kg^{-1}$ and 103 $mg{\cdot}kg^{-1}$, respectively. Mice treated with doses of **TLD-1411** higher than MTD_{50} showed sign of weakness, ataxia and died a couple of days post-injection. On the contrary, **TLD-1433** when given at higher doses than MTD_{50} did not cause death and all behavioural symptoms disappeared 24 h post-injection. Accumulation studies showed that both compounds were detectable in the tumour, liver and brain after 24 h. Tumour concentration of **TLD-1411** was lower than the one of **TLD-1433** (4.32 μM to 16.1 μM). The efficacy of PDT treatment was also tested using the same mouse model. Mice with grown tumours were injected with compounds and irradiated after 4 h thereafter with 190 $J{\cdot}cm^{-2}$ for 32 min in 30 s cycles. Tumours were significantly reduced when treated with 2 $mg{\cdot}kg^{-1}$ of **TLD-1411** and displayed a growth delay of 8 days. However, all tumours recurred. A higher dose of 5 $mg{\cdot}kg^{-1}$ of **TLD-1433** gave a tumour reduction and growth delay of 9 days. The researchers also checked whether continuous wave (cw lasers) or pulsed lasers would give better results with the tested PSs. Cw lasers are regularly used in PDT applications. Pulsed ones have the advantage of lowering down the local tissue heating, keeping the high power density. Mice treated with **TLD-1411** and **TLD-1433** showed significant increase in survival when higher doses of the compounds as well as cw light source was applied.

Upregulated receptors or cell surface markers in cancer cells are useful targets for therapeutic agents. Usually, targeting mosaic is conjugated with the complex. It is also common to use the association of the serum or membrane proteins with the active compound in non-covalent

manner to improve compound uptake. Ru complexes are known to associate with human serum albumin (HSA) or transferrin.[19, 20] Transferrin is a 78 kDa glycoprotein necessary for chelating Fe^{3+} from the serum.[21] Cancer cells display upregulated levels of transferrin receptors due to their higher demand for Fe^{3+} to grow.[22] In 2016, Lilge *et al*. confirmed that the uptake of **TLD-1433** as well as ROS production upon light irradiation (96 laser diode array light source; 625 nm; 90 ± 6 J cm^{-2}) were improved in cell free environment when the complex was mixed with transferrin.[23] **TLD-1433** associated with transferrin showed also lower dark cytotoxicity, probably due to enhanced Fe^{3+}delivery to the cancer cells, and resistance to photobleaching in contrary to **TLD-1433** alone.

Cell localisation of **TLD-1433** and its impact on cell metabolism by changing the cellular redox balance was published in a recent study.[24] Colocalisation studies performed by confocal and time-resolved laser scanning microscopy were inconclusive. Additionally, fluorescence signals of the tracking dyes vanished before the **TLD-1433** signal could be detected. It is possible that redox reactions and complex activation during laser scanning could be the reason for that unexpected phenomena.

The good results obtained with **TLD-1433** led to the preparation of a series of cyclometalated Ru(II) complexes similar to **TLD 1433** structure (**1-4**, Figure **3**).[25]

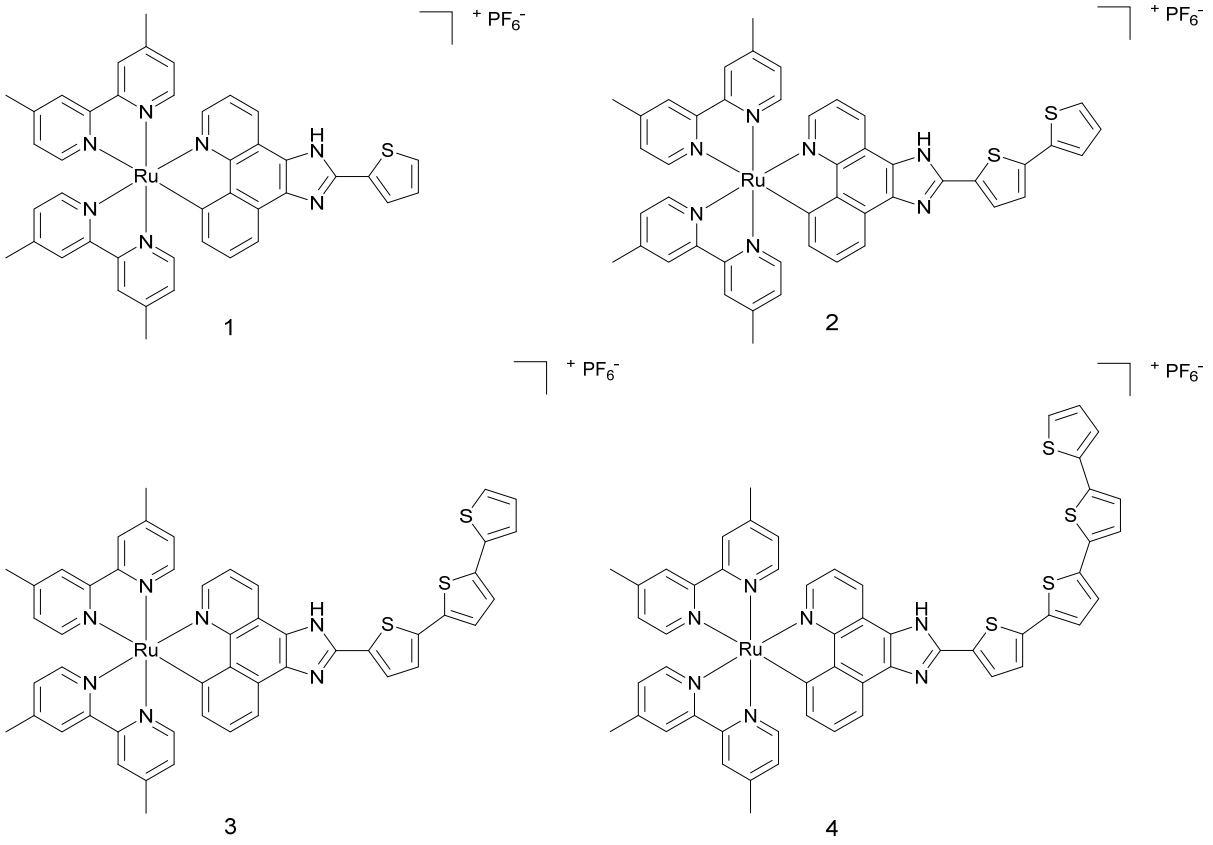

Figure 3. Structure of complexes **1-4**

Cyclometalated Ru(II) complexes are usually more photostable and their absorption spectra is red-shifted compared to diamine Ru(II) complexes. The (photo-)toxicity of the complexes was checked in two cell lines, namely SK-MEL-28 (melanoma) and CCD-1064Sk (normal skin fibroblasts). Complexes **1-3** were found to be highly cytotoxic in the dark towards melanoma cell line and were affecting much less normal skin fibroblasts. Complex **4** did not show any cytotoxicity in the dark. Upon irradiation with visible light (400-700 nm, 34.7 $mW{\cdot}cm^{-2}$), all complexes appeared to be extremely cytotoxic to melanoma cells. Particularly, complex **4** had a surprising PI of more than 1100, much higher than the three other complexes. To determine if complexes **1-4** would possibly bind to DNA, a mobility shift assay was performed. Upon light irradiation with visible light, the pUC19 plasmid formed aggregates in the presence of the complexes. No single-strand nor double-strand DNA breaks were observed under these conditions. Ethidium bromide staining with or without light irradiation was impaired,

presumably as a result of the intercalation of complexes **1-4** into DNA, or quenching of the ethidium bromide fluorescence. Confocal microscopy and DIC images were taken to assess compounds uptake and cells morphology before and after light treatment (400-700 nm, 34.7 $mW \cdot cm^{-2}$, 50 $J \cdot cm^{-2}$). Complexes **1** and **2**, which had the highest uptake in melanoma cells, as determined by confocal microscopy, were not taken up by non-cancerous cells. Complexes **3** and **4**, despite their lower uptake in melanoma cells, caused impressive changes of cell shape upon light irradiation, contrary to complexes **1** and **2**.

Mitochondria targeting compounds

Mitochondria are the cell energy centres and play and important role in the intrinsic apoptotic pathway. DNA damage, metabolic stress or the presence of unfolded proteins might lead to the permeabilisation of mitochondrial outer membrane. The release of mitochondrial proteins into the cytosol (e.g. cytochrome *c*) activates an apoptotic signalling cascade and finally leads to cell death.[26] Generation of singlet oxygen or other ROS in this organelle might trigger a rapid apoptotic response in the targeted cell, making this cellular compartment an interesting target for PDT photosensitizers.

Two Ru(II) polypyridyl compounds that target mitochondria functionalized with tyrosine and tryptophan were designed in 2013 (Figure 4).[27] Both amino acids were chosen to improve the cellular uptake of the Ru complexes.

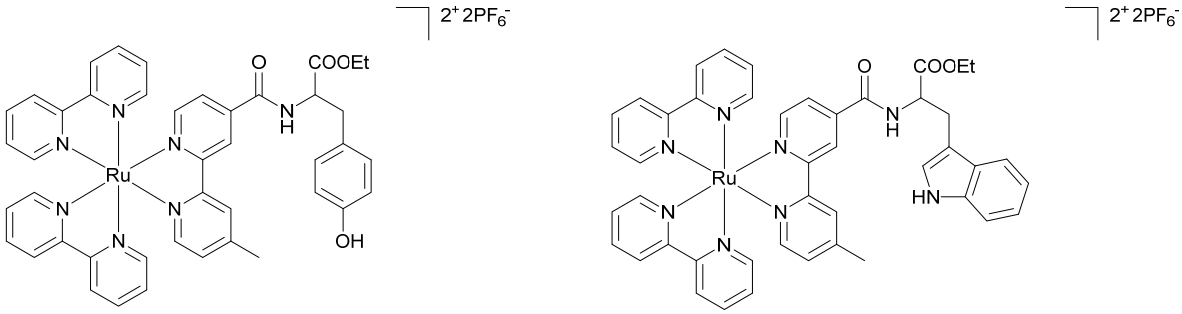

Figure 4 Structures of complexes **5** and **6**.

Cytotoxicity in the dark and upon light irradiation (4 h with visible light source λ~450-480 nm, 10 J cm^{-2}) of both compounds was examined in A549 (pulmonary carcinoma) and HCT116 (colon cancer) cell line. Promising phototoxic index (PI) values in A549 cell line (>10 for complex **5** and >10 for complex **6**) and in HCT116 (>9 and >10, respectively) encouraged the authors to perform further biological studies.

Singlet oxygen $^1O_2$ production upon light irradiation was confirmed and was suggested to be responsible for cell death. Fluorescence spectroscopy, UV-Vis absorption and isothermal titration calorimetry experiments showed that the Ru(II) complexes were able to bind CT-DNA in a non-covalent way, probably by intercalation into the DNA groove. Irradiation of pUC19 plasmid with the Ru(II) complexes led to photo-cleavage of the DNA, suggesting this mechanism as the main cause of cell death. This finding was further confirmed by single cell gel electrophoresis, which revealed DNA damage in treated A549 cells upon light irradiation. Confocal laser scanning microscopy helped identify the cellular localisation of the complexes in A549 cells. Unexpectedly, none of the compounds was found to localise in the cell nucleus. Signals from Mitotracker Green suggested the presence of the complexes in mitochondria and cell membranes. Microscopy studies after light irradiation would have been an interesting addition to the work since some of the compounds are known to modify their localisation after illumination of the cells.[28] Nevertheless, singlet oxygen is known to alter the mitochondrial trans-membrane potential, which might trigger the apoptotic pathway. To further investigate the molecular mechanism of cell death, western blot analysis was performed. It revealed that caspase-3, a marker of apoptosis, was found to be overexpressed in irradiated cells. The researchers concluded that the mechanism of cell death included the disruption of mitochondria membrane potential that, in turn, triggered the caspase-3-dependent apoptotic pathway.

Biological evaluation on Ru(II) complexes containing pdppz ([2,3-h]dipyrido[3,2-a:2',3'-c]phenazine) ligands was published in 2015.[16] Complexes 7 and **8** were expected to bind DNA because of their extended dppz ligand, while complex **9** was used as a control (see Figure 5 for chemical structures). Experiments confirmed that complexes 7 and **8** were able to intercalate DNA in non-cell environment. Incubation of complex **8** with the plasmid pBR322 upon light irradiation (390nm, 2 J cm^{-2}) caused single and double breaks in the DNA. Such effect was not seen with complex **7**. It was shown that HeLa cells could actively uptake compounds **7** and **8**-

in a temperature-dependent manner. Confocal microscopy studies of complex **8** demonstrated that this compound colocalised with mitochondria and lysosomes, which clustered near the nucleus. It is possible that small amounts of **8** were also able to localise to the nucleus. Alkaline comet assay revealed DNA damage in treated and irradiated cells. ICP-MS experiments would have been an attractive addition to this study.

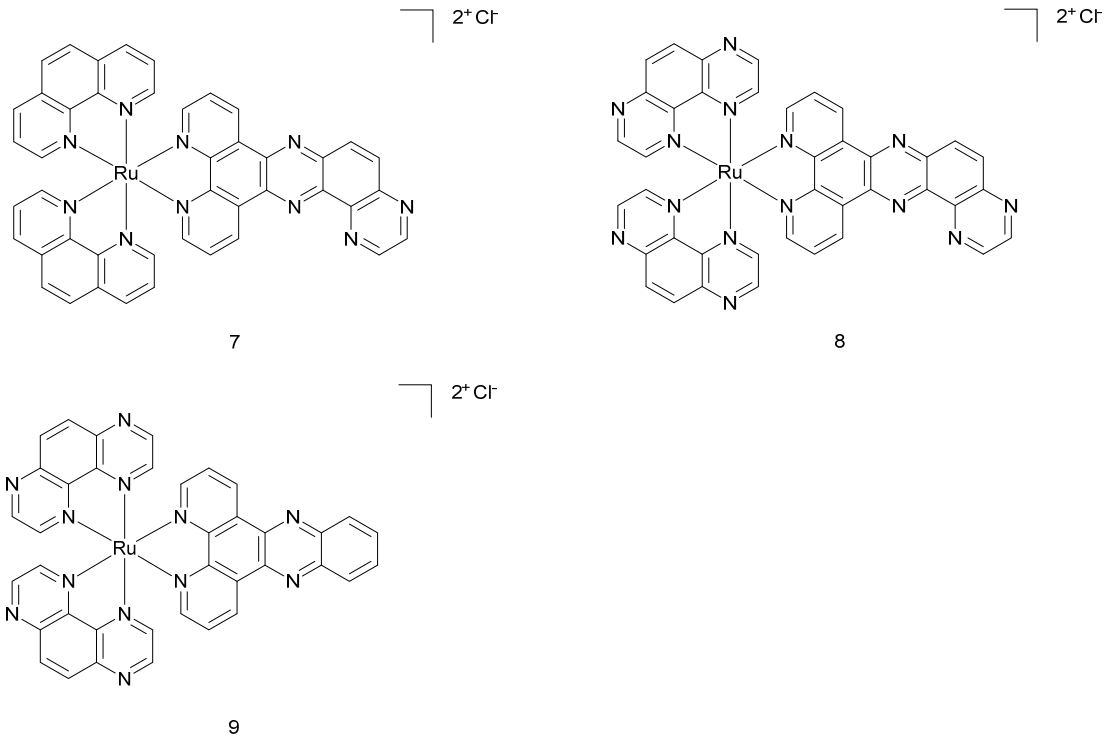

Figure 5. Chemical structures of complexes **7**, **8**, **9**.

Cytotoxicity of the complexes in the dark and light conditions (≥400 nm, ~18 J cm^{-2}) was examined in HeLa (cervical cancer), two mesothelioma cell lines (CRL5915 and One58), in Mutu-1 (Epstein-Barr virus-related Burkitt lymphoma) and DG-75 (Burkitt lymphoma) cell lines. Complex **7** did not show any dark or light cytotoxicity. Complex **8** was moderately cytotoxic in the dark (Inhibitory concentration 50 -IC_{50} values ranged from >100 to 40.2 μM). Light irradiation of the treated cells caused phototoxic effect (IC_{50} values ranged from 42.8 to 8.8 μM). Pre-treatment of Hela cells with N-acetylcysteine (NAC), an established antioxidant, confirmed that ROS were involved in cell death. Hela cells were 50% more viable with the

NAC treatment upon light irradiation. Real-time confocal microscopy demonstrated that HeLa cells treated with **8** displayed an apoptotic morphology upon light irradiation. Such result was confirmed by Fluorescent Activated Cell Sorting (FACS) analysis. Interestingly cell death could be prevented when cells were co-treated with VAD-fmk (inhibitor of caspases). Hence, these results demonstrated that **8** triggered apoptotic cell death in the treated cells.

Another set of four Ru (II) compounds that target mitochondria was synthesised by the Chao group in 2015 (see Figure 6 for structures).[29]

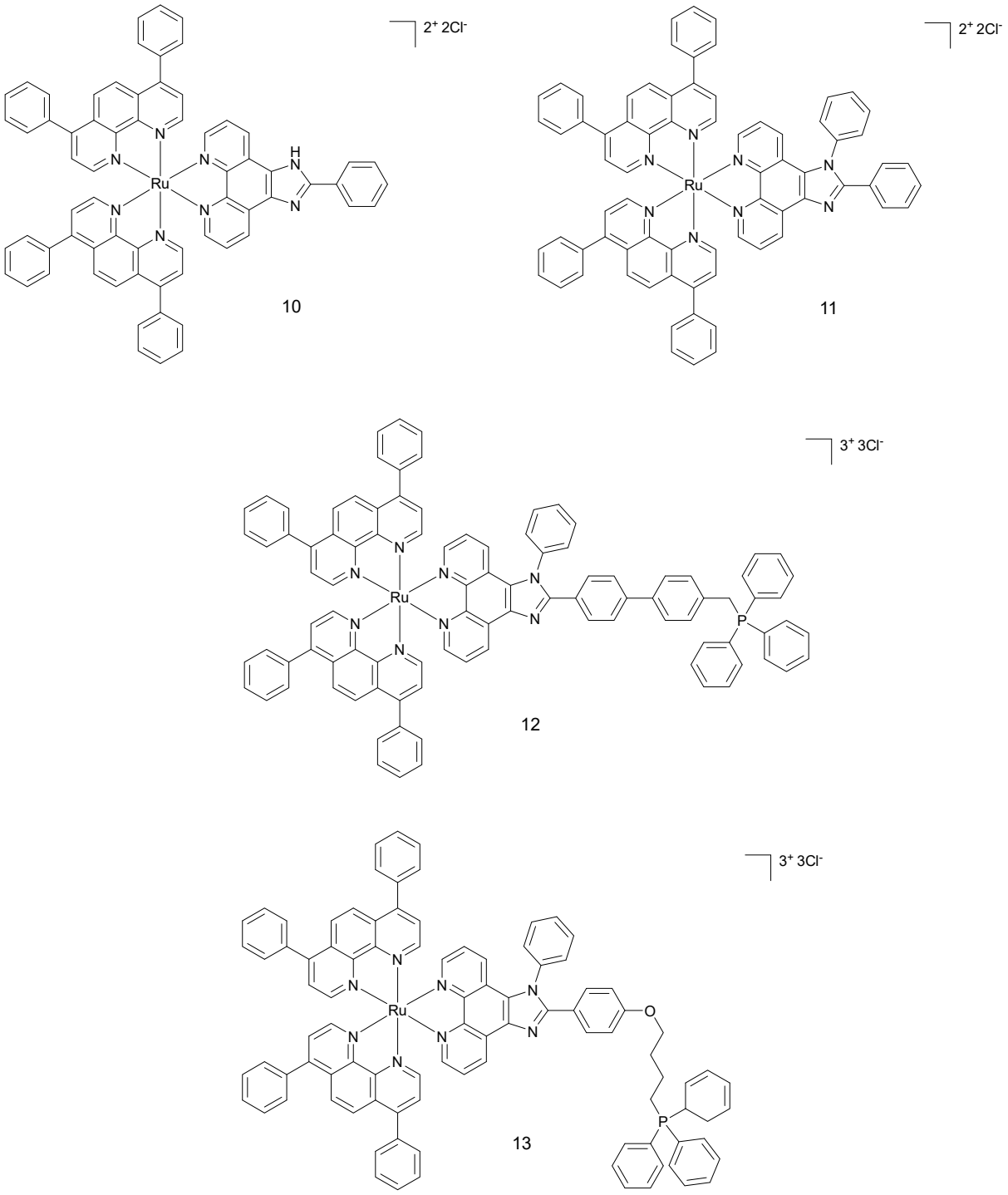

Figure 6. Chemical structures of complexes 7, 8, 9 and 10.

The triphenylphospine (TPP) present in complexes **12** and **13** adds lipophilic character to the compounds, resulting in better mitochondria targeting abilities.[30] Confocal microscopy with Mitotracker Green in HeLa cell line revealed that complex **13** localises in the mitochondria. Three other compounds were found to moderately localise in that compartment. Localisation

results were confirmed by ICP-MS analysis, showing that complexes **10-12** were present in higher amount in the cytoplasm (Figure 7).

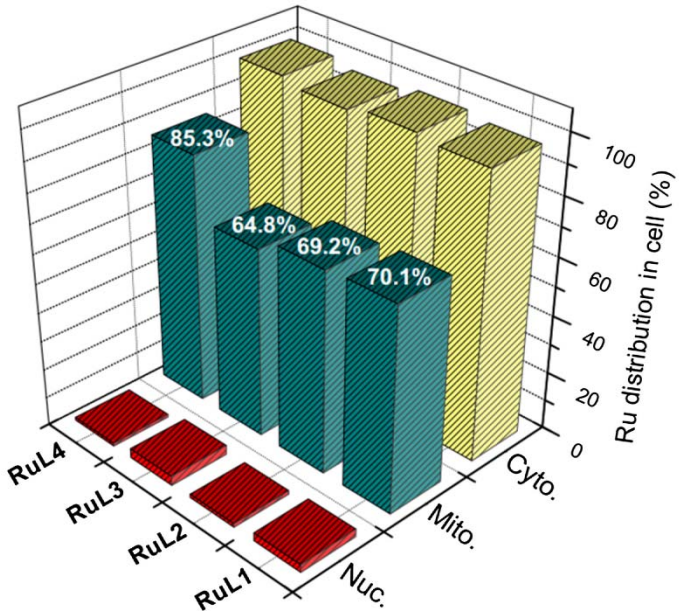

Figure 7. ICP-MS quantification of the internalized Ru by the HeLa cells. Figure taken from ref 30 with permission from Elsevier.

All four compounds were designed to produce singlet oxygen not only using a one-photon but also a two-photon irradiation process. Confocal microscopy images of Hela cells taken before and after two-photon irradiation (810-830 nm for 3 minutes; 800 $J{\cdot}cm^{-1}$) with 2,7-dichlorodihydro-fluorescein diacetate (DCFH-DA) allowed verifying singlet oxygen production in all samples. Dark and light cytotoxicities of all compounds were tested under one-photon irradiation. Compounds were not toxic under dark conditions (IC_{50} >100 µM). After irradiation (LED source; 450 nm; 12 $J{\cdot}cm^{-2}$), complexes **10-12** showed similar cytotoxicity, varying from 12.4 to 15.5 µM. Probably due to its high concentration in mitochondria, complex **13** was found to be the most effective compound tested, with a PI >28. Since monolayer cell cultures are not a good model for tumour treatment, HeLa multicellular tumour spheroids (MCTS) were used for further tests. Diffusion of the compounds (10 µM, 8 h treatment) was examined in 800 µm MCTSs. Treated spheroids were imaged with one-photon and two-photon

z-stack microscopy. The luminescence signal of the compounds was found in all depth sections of the spheroids. Two-photon microscopy showed deeper penetration of the complexes through spheroids than one-photon microscopy, probably due to its excitation wavelength in the therapeutic window. This confirmed the high permeability of the complexes through the MCTSs. Singlet oxygen generation with DCFH-DA was also investigated in MCTS. Enrichment of the singlet oxygen signal was observed in the treated spheroids. The results showed lower signal of produced singlet oxygen in the cores of the spheroids as compared to their surface. Compounds treatment also inhibited MCTSs growth after irradiation with two-photon technique. The best results were obtained again with complex **13**. All synthesised compounds exhibited good photodynamic therapy ability against the HeLa cell line. However, further investigations should include healthy cells to establish a possible therapeutic window for these compounds.

An interesting study was recently published by the same group, who designed mitochondria-localising Ru(II) complexes that can be activated by glutathione (GSH).[31] The aim of the study was to improve the tumour selectivity of the Ru complexes that are used as PDT PSs. Complex **14** is a dinuclear Ru(II) complex, which is bridged by a GSH activating ligand 4,4”-azobis(2,2’-bipyridine) (Figure 8). Specific properties of the ligand cause quenching of luminescence of the Ru complex. Since intracellular concentration of GSH in cancer cells are higher than in healthy ones, the authors were hoping that the complex would be activated and transformed into complex **15** (Figure 8), and this mostly in cancer cells.

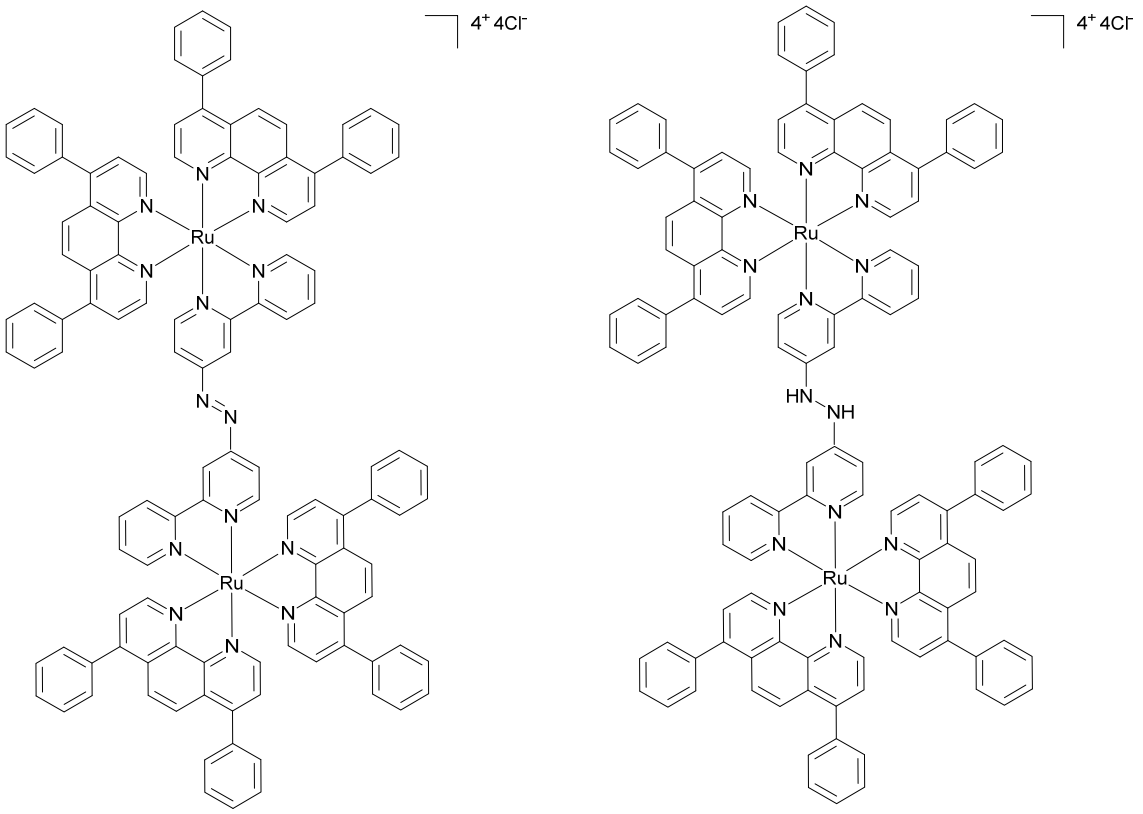

14 15

Figure 6. Chemical structures of complex **14** and complex **15**.

For the experiments, Chao and co-workers used two cell lines, namely HeLa and LO2 (human fetal hepatocyte- healthy control). Both were cultured in monolayers as well as in MTCSs. ICP-MS and confocal microscopy experiments confirmed that the mitochondria were the main target for complex **14**. As expected, LO2 cells displayed a much weaker accumulation of the complex compared to Hela. Two-photon irradiation (810 nm, 100 mW, 80 MHz, 100 fs) was used to establish ROS generation in treated 2D and 3D cell cultures. A strong green fluorescence of the ROS indicator was detected, confirming that the complex was able to permeate the MCTSs and induce single oxygen production. Cytotoxicity studies demonstrated that complex **14** was not toxic in the dark (IC_{50}> 70 μM) for both cells lines. After 15 min irradiation at 450 nm (20 $mW{\cdot}cm^2$), its cytotoxicity raised to about 5 μM for HeLa and 13 μM for LO2 cells. Similar results were obtained with cancer cell MCTSs. Complex **14** was not toxic in the dark (IC_{50} >

100 μM) and became more harmful on MCTSs after light irradiation (5.71 μM). Viability of the MCTSs was checked by Calcein AM staining. Irradiation of treated cells caused loss of the fluorescent signal from the dye, suggesting cell death. It is worth noting that MCTSs treated with complex **14** at 10 uM concentration stopped growing two days after two-photon irradiation, whereas the control group treated with the same concentration of cisplatin kept growing. Of note, annexin V and propidium iodide (PI) staining showed that apoptosis was the main cause of cell death.

In 2018, Stang, Chao and coworkers prepared a tetrametallic macrocyclic structure containing Ru(II) and Pt(II) atoms, that can be used in two-photon PDT (Figure 9).[32]

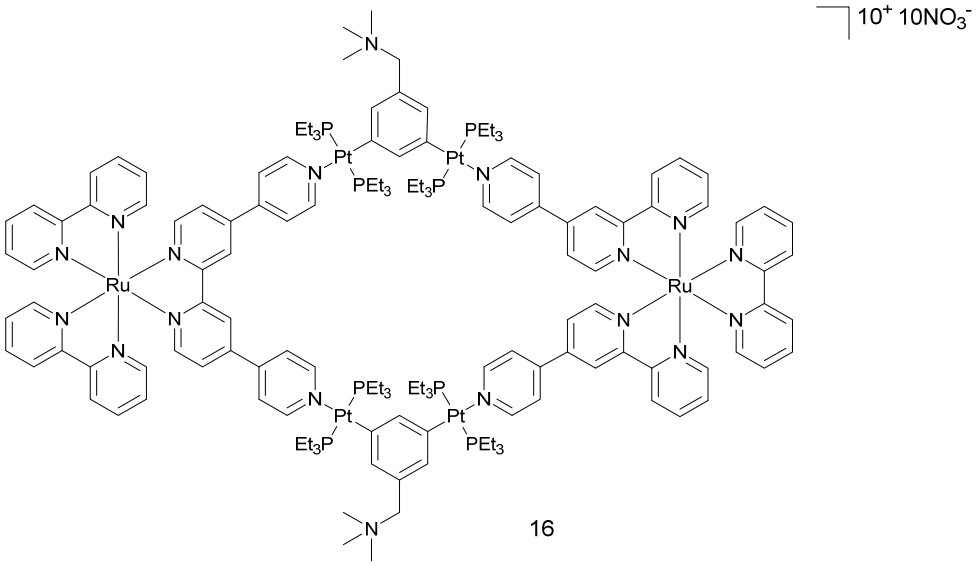

Figure 9. Chemical structures of complex **16**.

The addition of the Pt(II) moieties to the two Ru(II) complexes was made to enhance the intrinsic photophysical properties of the Ru(II) complexes. Impressive two photon absorption (TPA) cross-section values of 1371 GM were obtained, which were much higher than the one of $[Ru(bpy)_3]^{2+}$ itself (66 GM). Moreover, the intersystem crossing process was enhanced, which elevated the singlet oxygen quantum yield value to 88% in mehanol, when $[Ru(bpy)_3]^{2+}$] was used as reference. Cellular localisation showed that metallacycle complex was

accumulating in the mitochondria and the nucleus. ICP-MS results corroborated those of microscopy, indicating that, after 2 h incubation, complex **16** (5 μM) localised in mitochondria (67 %) and in the nucleus (25 %). Cellular uptake data revealed that complex **16** entered the cells through endocytosis pathway. Cytotoxicity experiments were performed on HeLa, A549, A549R (cisplatin resistant cell line), KV (multi-resistant human oral floor carcinoma) and PC-3 (prostate cancer) cell lines. The PI values ranged between 11.6- 114 (irradiation conditions: LED source; 450 nm, 21.8 mW cm^{-2}, 5 min). Since A549 cells displayed the highest PI, they were chosen as a model cell line for further studies. DCFH-DA staining and calcein AM/ethidium homodimer-1 (EthD-1) co-staining after two photon (TP) irradiation of the treated cells confirmed that compound **16** can generate singlet oxygen and cell death only in the irradiated area. Compound **16** caused cell apoptosis, confirmed by annexin V and PI staining as well as by elevated levels of caspase-3/7. To assess the impact of complex **16** in mitochondria and nucleus, several tests were performed. The mitochondrial membrane potential (MMP) was significantly lower in irradiated cells. TP irradiation also caused DNA fragmentation in the nucleus. Due to these promising results obtained *in vitro*, *in vivo* studies in mice were performed. To assess two photon photodynamic therapy (TP-PDT) efficacy of complex **16**, A549 tumour bearing nude mice were used. The group treated with complex **16** (0.5 mg kg^{-1}) and irradiated with TP laser (800nm, 50 mW, 20 s mm^{-1}) did not exhibit observable weight loss. The tumour volume of the treated group was reduced by 78%, while control mice groups showed 13-fold increase in tumour mass. Additionally, examination of tumour tissue of the treated group showed pathological changes, which were not observed in other organs like liver, kidney, heart, etc.

Nucleus targeting compounds

Besides mitochondria, another important target for PDT PSs is the nucleus. Generation of singlet oxygen or other ROS, in close proximity to the DNA, might allow for DNA damage, and finally lead to cell death. It is known that dipyridophenazine (dppz) ligands have the ability to intercalate within DNA.[33, 34] That is why in 2014 six different $[Ru(bpy)_2dppz]^{2+}$ derivatives **17-22** were investigated by our groups (Figure **10**).[35]

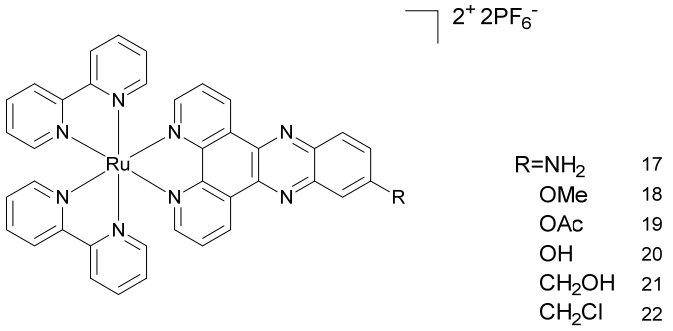

Figure 10. Chemical structures of $[Ru(bpy)_2dppz]^{2+}$ derivatives.

Singlet oxygen production study showed that all compounds had a high efficacy for $^1O_2$ production but only in hydrophobic environment. The excited state of the complexes bearing a dppz ligand are quenched very fast in the presence of water molecules.[36] All synthesised complexes were found to be non-cytotoxic in the dark (IC_{50} >100 μM) against HeLa and MRC-5 cells (normal lung fibroblast). Light cytotoxicity studies were performed using two different light treatments: 10 min at 350 nm (2.58 $J \cdot cm^{-2}$) and 20 min at 420 nm (9.27 $J \cdot cm^{-2}$). Among all compounds, only complexes **17** and **18** showed an interesting phototoxic effect. The PI value for complex **9** was higher than 150, while for complex **18** it was 42. The cellular uptake of the Ru compounds was investigated by High-Resolution Continuum Source Atomic Absorption Spectrometry (HR-CS AAS), showing that it correlated well with toxicity studies. The most cytotoxic complexes **17** and **18** had the highest accumulation in the HeLa cells (1.08 and 1.76 nmol Ru per mg protein). Accumulation of the compounds in the MRC-5 cell line was different

since only 0.76 and 0.18 nmol Ru per mg protein were determined. This indicates that the complexes penetrated the non-cancerous cell line to a lesser extent than the cancerous line. Cellular localisation of complexes **17** and **18** was investigated using confocal microscopy.

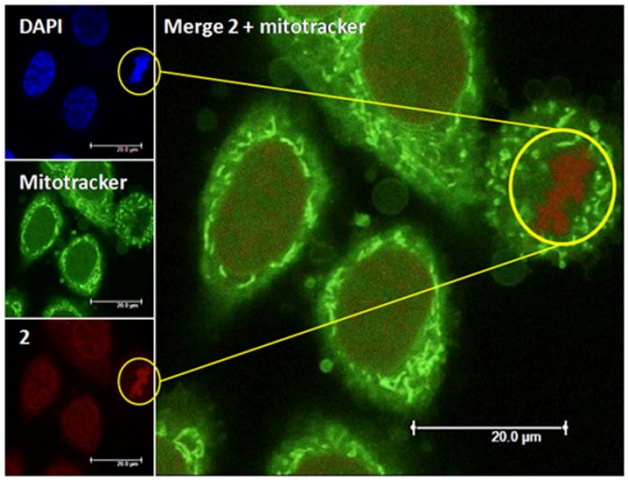

Figure 11. Cellular localisation of complex **18.** Figure taken from ref 36, with permission from John Wiley and Sons.

The first complex was difficult to detect even when cells were treated with high doses of compound. The low luminescence quantum yield is probably responsible for this result. On the other hand, complex **18** was able to accumulate preferentially in the nucleus. Because of the luminescent quenching effect of the complex in aqueous environment mentioned above, fluorescence microscopy localisation was supported by HR-CS AAS. The results showed that both complexes efficiently accumulated in the nucleus (0.43 ± 0.05 and 0.96 ± 0.06 nmol Ru per mg protein). To check if nuclear localisation and binding to DNA might have been the reason of toxicity, DNA photocleavage experiments were conducted. Treatment of pcDNA3 plasmid with complexes and irradiation at 420 nm for 20 min (9.27 $J \cdot cm^{-2}$) showed that both complex **17** and **18** were able to cleave plasmid DNA. Administration of compounds in the dark did not cause cleavage of the plasmid. In a follow up study, our groups further explored the molecular cell death mechanism of complex **18.**[37] Mechanistic studies on the outcome of DNA binding led to the conclusion that irradiation of the intercalated compound caused oxidative

damage of purines in DNA. Importantly, alkaline comet assay supported these results in living cells. Confocal microscopy images of different cell lines such as U2OS (human bone osteosarcoma), MCF-7 (mammary gland adenocarcinoma) and RPE-1 (normal retina pigmented epithelium) confirmed that the complex was mainly localised in the nucleus [35]. ICP-MS confirmed these results. The determination of the presence of specific markers of DNA damage response, analysis of DNA content and cytotoxicity studies after irradiation showed that cells underwent cell cycle arrest and loss of viability. Annexin V and PI staining experiments of interphase cells excluded classic apoptotic or necrotic cell death. Further analysis demonstrated that cell death was caused by DNA damage and endoplasmic reticulum-(ER) mediated stress response pathways. On the other hand, treatment and irradiation of mitotic cells caused death according to classic apoptotic pathways, indicating two distinct modes of cells death in interphase or mitosis and pointing to the potential of the use of these compounds in combination with established cancer therapeutics.

Further studies on Ru(II) polypyridyl complexes with dppz ligands were performed by our group in collaboration with the Chao group.[28] Two substitutionally inert complexes, namely $[Ru(phen)_2(dppz\text{-}7,8\text{-}(OMe)_2]^{2+}$ (complex **23**) and $[Ru(phen)_2dppz\text{-}7,8(OH)_2]^{2+}$ (complex **24**) were investigated (see Figure 12 for structures).

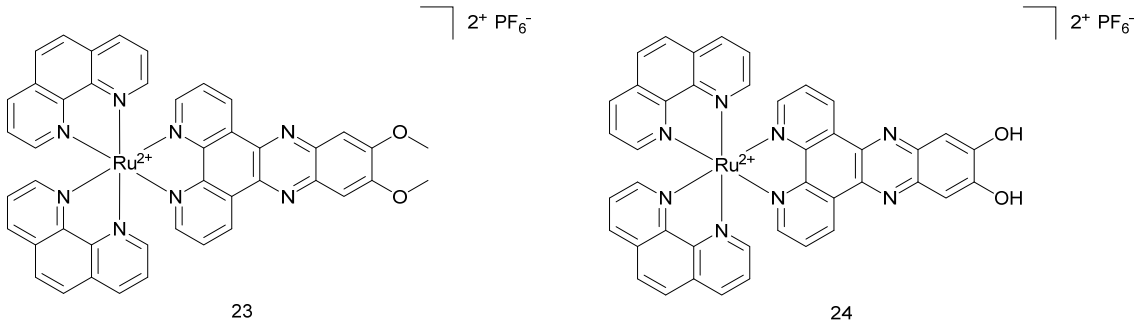

Figure 12. Chemical structures of complex **23** and complex **24**.

The aim of this study was to investigate if small structural differences could cause significant changes in the biological response. It is worth noting that both complexes were investigated for use in one-photon (OP) and two-photon (TP) PDT. Dark and light cytotoxicity studies on HeLa and MRC-5 cell line monolayers showed that the introduction of -OMe groups on the ligand enhanced toxicity compared to those bearing the -OH groups (decrease of the IC_{50} value from 16.7 ± 2.6 μM in -OH bearing compound to 3.1 ± 0.6 μM in -OMe compound in HeLa). Both complexes were also much more effective than the positive control aminolevulinic acid (5-ALA), an approved PDT PS. Interestingly, the compounds were also studied on 3D multicellular tumour spheroid to provide a comprehensive overview on how Ru(II) complexes might act in solid tumours. Surprisingly, only complex **23** was active on MCTSs upon light irradiation (LED light source; IC_{50} 32.5 ± 6.8 μM). To further explore the mechanism of action of the complexes, cellular localization and uptake of the compounds were studied. ICP-MS showed that the amount of complex **23** was much higher in HeLa cells than complex **24** (2.4 nmol Ru/mg protein to 0.9 nmol Ru/mg protein). This result might explain the differences between the IC_{50} values obtained for both complexes in the dark and upon light irradiation. Confocal microscopy showed that the Ru complexes under study localised in different compartments of the cell. Complex **23** was found to accumulate in the nucleus and mitochondria while **24** localised in the outer cell membranes. Imaging was also performed after light irradiation. Complex **23** changed its localisation and moved completely into the nucleus, probably as result of damage generated by singlet oxygen in membranes, enabling the compound to reach the nucleus. Worthy of note, these Ru complexes might also localise in other compartments that escaped detection by confocal microscopy. Indeed, due to luminescence quenching in aqueous solution of these dppz-containing complexes, their detection is only possible in hydrophobic environment.[38] OP and TP absorption was also used to image both compounds in spheroids. For both complexes, TP imaging gave better results. In

this experiment, complex **23** completely permeated the MCTSs, while complex **24** could only be detected in the external parts of the spheroids (Figure 13 and Figure 14).

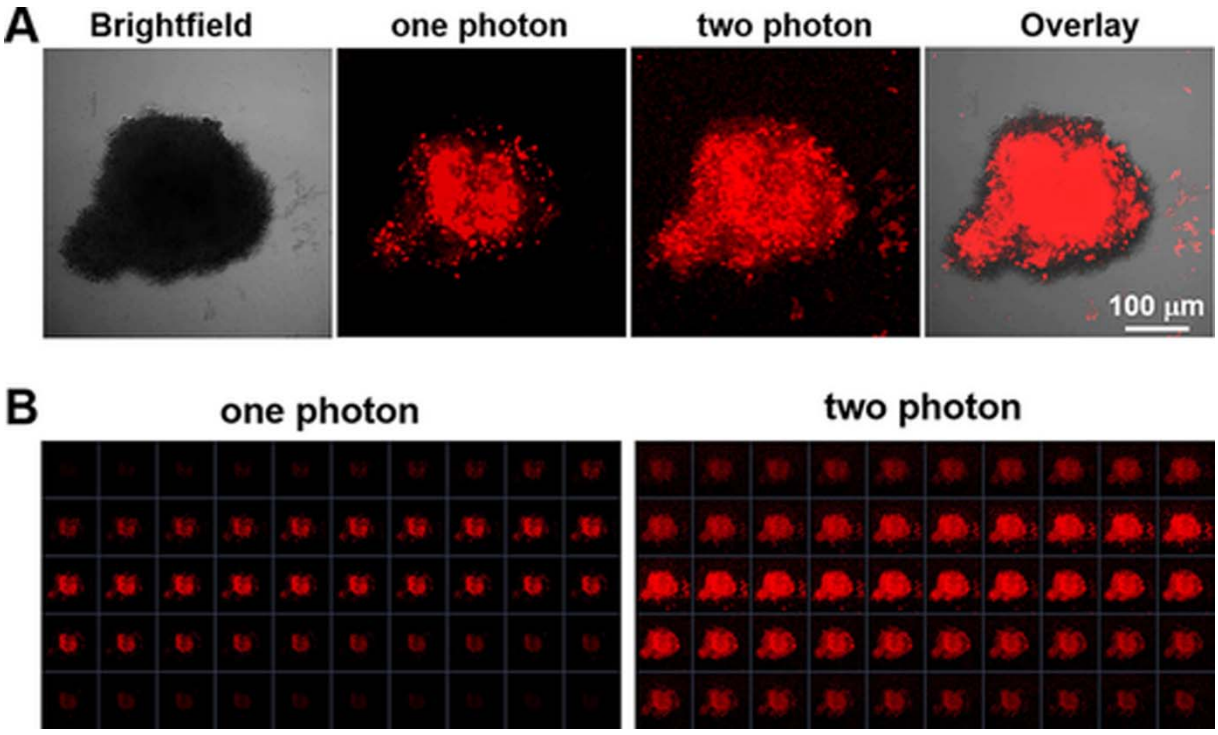

Figure 13. A. OP and TP images of **23** after incubation with HeLa spheroids for 12 h.

B stack images of the same HeLa spheroids captured every 5 µm along the Z-axis.

Figure taken from ref. 29 with permission from John Wiley and Sons.

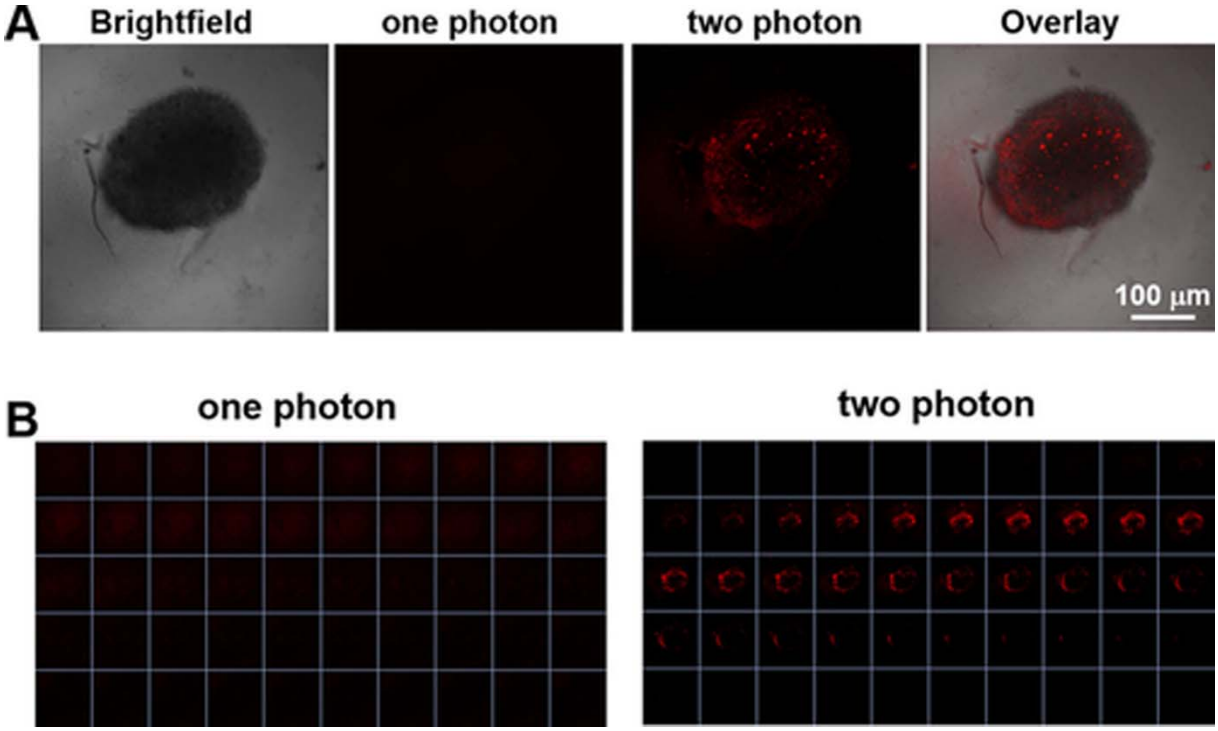

Figure 14. A. OP and TP images of **24** after incubation with HeLa spheroids for 12 h. B stack images of the same HeLa spheroids captured every 5 µm along the Z-axis. Figure taken from ref. 29 with permission from John Wiley and Sons.

Comparable results with structurally related compounds were obtained by the Glazer group in 2014.[39] Although complexes **25** and **26** have very similar photophysical properties (Figure 15), the differences in their overall charge and hydrophilicities led to distinct biological effects. While complex **25** localised in the mitochondria, complex **26** did not show specific organelle localisation and was found in the cytosol. Upon irradiation (30 s pulses; >400 nm; 7 $J \cdot cm^{-2}$), complex **25** caused necrotic cell death distinct from complex **26** which turned on the apoptotic pathway. It is possible that the addition of sulfonic acid groups on complex **26** induced a different cell localisation and consequently a different type of cell death.

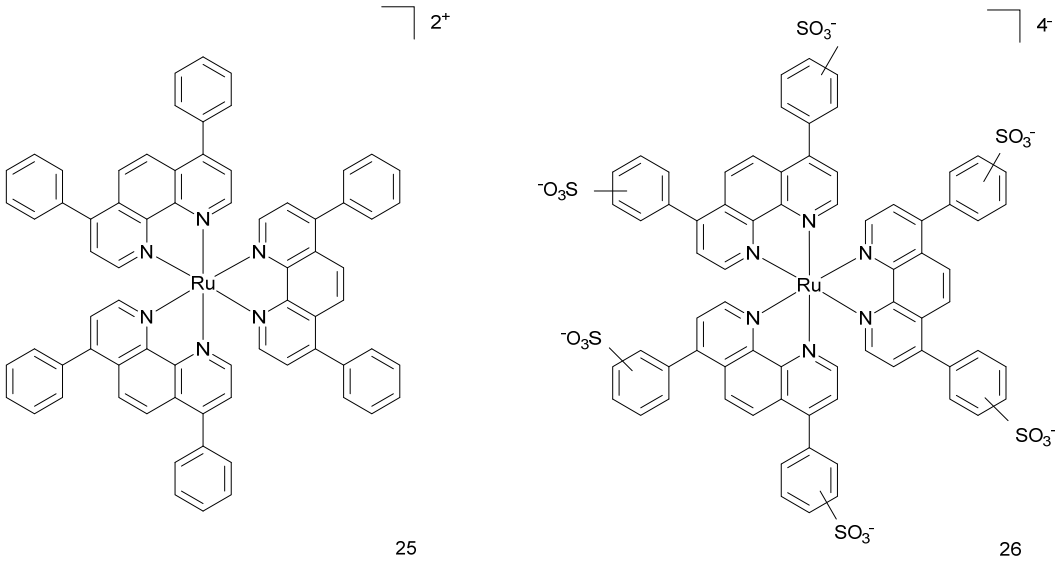

Figure 15. Chemical structures of complex **25** and **26**.

Similar conclusions were brought in 2015, when small changes in the structure of Ru(II)-based PSs cancelled phototoxicity of the complex.[40] In this case, two inert Ru(II) polypyridyl complexes with a nitrile containing ddpz ligand and two bypridine or phenantroline ancillary ligands were tested. In contrast to previously described Ru(II) complexes with dppz ligands, both did not exhibit high singlet oxygen production (20% comparing to 50%-90%). This is probably why these complexes did not display any cytotoxic effect upon light irradiation (RPR 200 Rayonet chamber reactor; 420 nm; 9.27 $J \cdot cm^{-2}$).

A series of four cyclometallated Ru(II) complexes with π-expansive ligands were described by McFarland in 2015 (Figure 16).

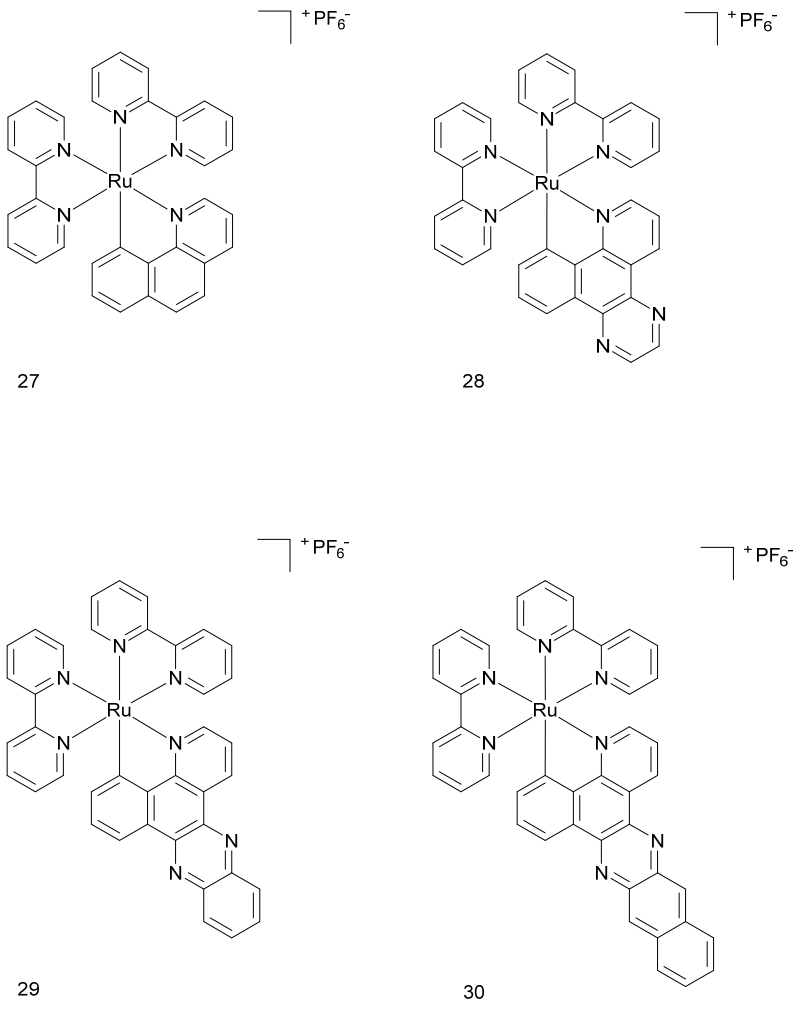

Figure 16. Chemical structures of complex **27-30**.

Cytotoxicity of the compounds was assessed in HL-60 (acute myeloid leukemia) and SK-MEL-28 cell lines. Complexes **27-29** were toxic to the cells in the dark and did not show high PI value (4-18) after irradiation (190 W BenQMS 510 overhead projector; visible light 400-700 nm; 34.2 $mW \cdot cm^{-2}$). On the contrary complex **30** showed an astonishing PI value, namely 1400. To assess if the complexes can interact with the DNA, a photocleavage assay was used. It was shown that all complexes could impair ethidium bromide staining due to induced DNA aggregation and precipitation. Because complex **30** was the most promising one, further tests were performed with it. Since **30** was generating singlet oxygen very weakly (less than 0.56% relative to $[Ru(bpy)_3]^{2+}$, it was suggested that the other ROS is responsible for the phototoxic effect in cells. Indeed, tests with dihydroethidium (DHE) in HL-60 cells confirmed that

superoxide $O_2^{\bullet-}$ was responsible for cell death. It was also shown in SK-MEL-28 cells that complex **30** altered its localisation upon light irradiation (from nucleus to cytoplasm) and induced morphology changes in the cells.

Lysosome targeting compounds

In 2015, our group in collaboration with the Chao group introduced highly charged homoleptic complexes that are suitable for TP-PDT (see Figure 17).[41]

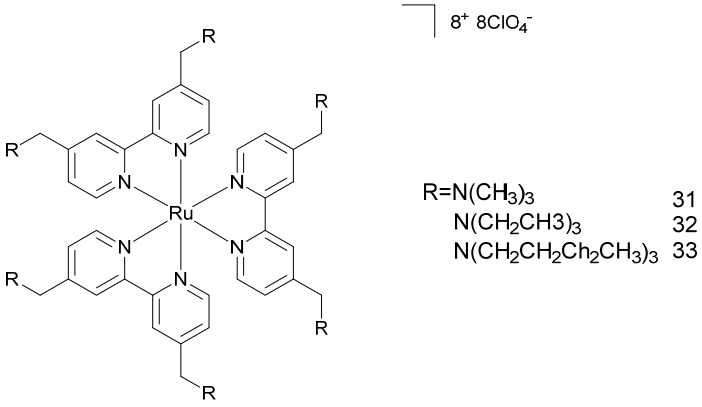

Figure 17. Chemical structures of highly charged complexes.

The compounds were found to be photostable and did not break down in bovine plasma. Electron paramagnetic resonance (EPR) experiments demonstrated that the main type of ROS generated by the three compounds at 450 nm irradiation was $^1O_2$. Cellular localisation of complexes **31**, **32** and **33** was determined using confocal laser scanning microscopy in HeLa cell line monolayers as well as in HeLa multicellular tumour spheroids. All three complexes were found to localise in the lysosomes, probably entering the cell by endocytosis pathway. ICP-MS experiments confirmed the microscopy outcomes. All compounds were not cytotoxic in the dark. After OP irradiation (450 nm, 10 $J \cdot cm^{-2}$), complex **31** showed particularly high phototoxicity with IC_{50} value of 1.5 μM (PI 313). All complexes had a higher phototoxicity than 5-ALA, which was used as a control PS. The same trend was also observed for MCTSs. Further investigations were performed with complex **31**, which was found to be the most promising compound of the series. Calcein AM staining and ROS indicator staining (DCFH-DA) showed that cell death was only limited to the place of irradiation. Morphology studies after TP light treatment showed that cells underwent shrinking and formed bubbles.

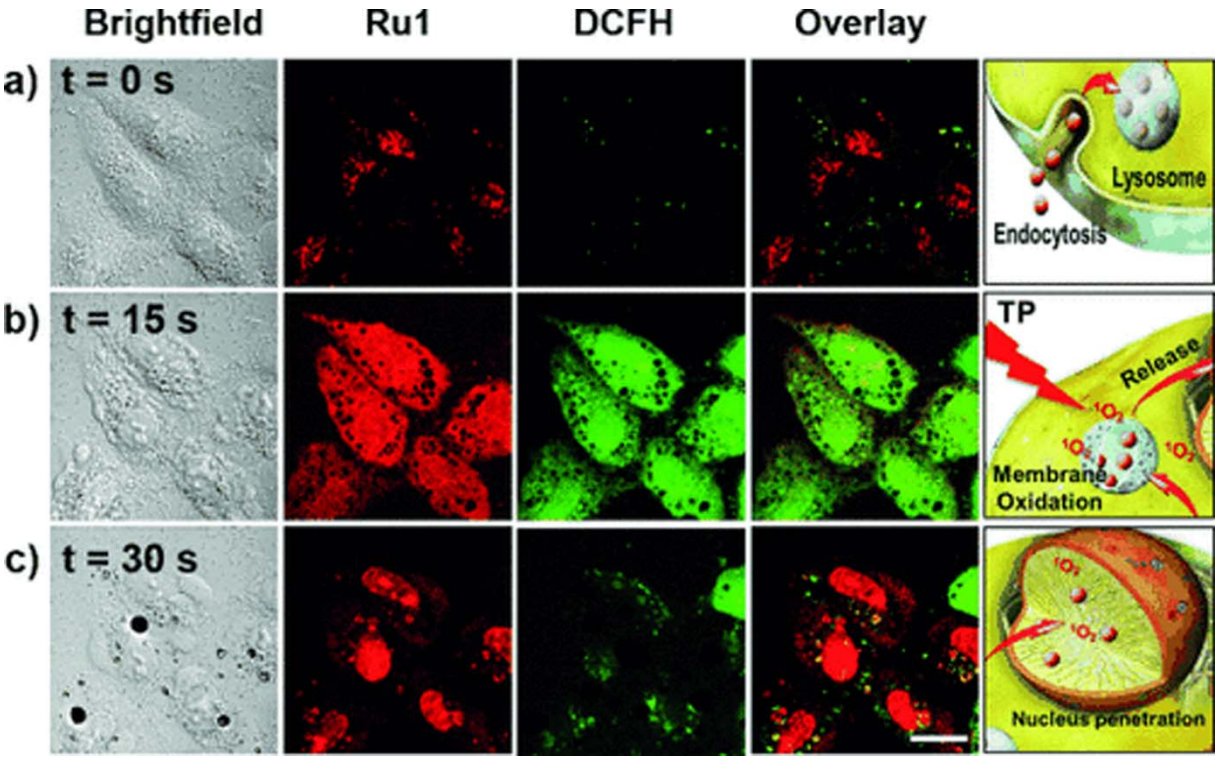

Figure 18. Micrographs of and ROS generation in HeLa cells incubated with complex **31** after irradiation with a two-photon confocal laser. Figure taken from ref. 42 with permission from John Wiley and Sons22

The cellular localisation of complex **31** was also altered. After irradiation, the compound was found in the cytoplasm, nucleus and nucleoli (see Figure 18). Microscopy analysis indicated that cells died by a necrotic process, bursting their content into the extracellular space. Overall, this investigation revealed that lysosomes might be a good target for future PDT PSs.

Targeting conjugates

The need for new Ru(II) polypyridyl complexes with better selectivity towards cancer cells led to the design of compounds with tumour specific targeting moieties. Such moieties might be antibodies, cell surface receptors, aptamers, etc.[42, 43] In 2015, Weil and Rau introduced a Ru(II)-based PS that was conjugated to somatostatin,[44] a peptide hormone produced by δ-cells of the pancreas inhibiting the release of insulin and glucagon.[45] Somatostatin receptors are frequently overexpressed in many tumour cancer cells, making them a good target for anticancer agents.[46] In this study, $[Ru(byp)_3]^{2+}$ derivative was conjugated to the peptide hormone to form complex **34** (Figure 19).

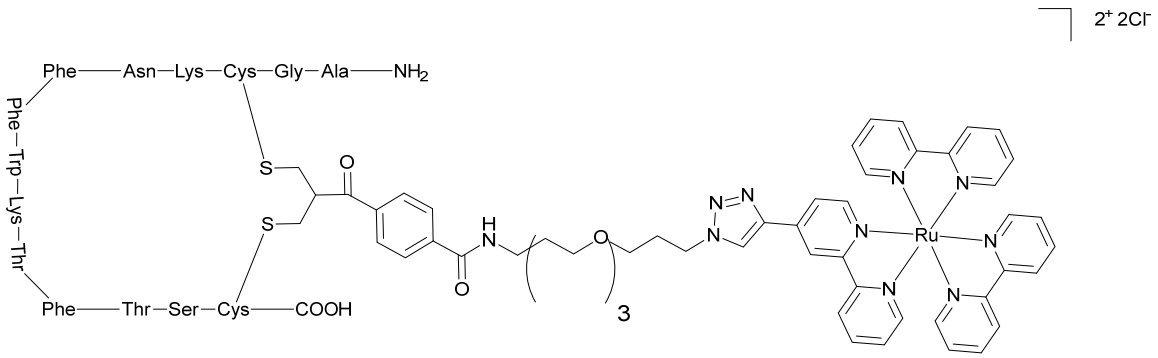

34

Figure 19. Chemical structure of complex **34**.

The cellular uptake of the conjugate was analysed by laser scanning confocal microscopy in A549 cells, which express different types of somatostatin receptors. The intensity of the compound emission was measured. A hundred times higher uptake of the somatostatin conjugate compared to the control was observed. Tumour selectivity was tested on wild type CHO-K1/Ga15 (Chinese hamster ovarian epithelial cell line expressing Gα15 alpha subunit protein) and cells overexpressing somatostatin receptor 2, CHO-K1/Ga15/SSTR2. Very high selectivity towards receptor overexpressing cells was confirmed by functional calcium flux

assay. The IC_{50} value for cytotoxicity by complex **34**, after light irradiation of A549 cells (LED array; 470 nm for 5 min; 6.9 ± 0.9 $J \cdot cm^2$), was 13.2 ± 1.1 μM. Interestingly, the compound did not show any dark cytotoxicity up to 300 μM.

A different approach was utilised by the same research groups two years later, when a Ru(II) complex was conjugated to a protein carrier scaffold containing mitochondria targeting groups to yield complex **35** (see Figure 20 for Ru(II) complex structure).[47]

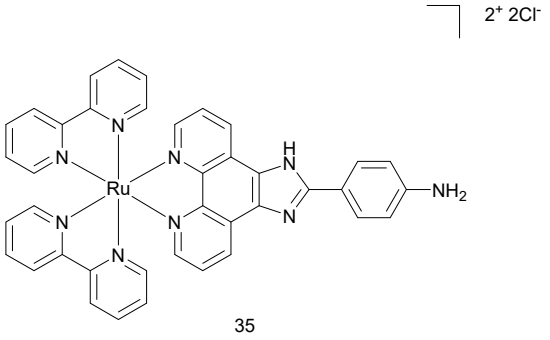

Figure 20. Chemical structure of Ru(II) complex that was conjugated to the protein carrier scaffold.

In this case, human serum albumin was the nanotransporter for the PS. Complex **35** was found to localise in mitochondria of Hela cells within 240 min, thanks to the TPP-mitochondria targeting groups. An impressing PI value of 250 was determined for the conjugate after irradiation for 5 min (LED array; 470 nm, ~ 20 $mW \cdot cm^{-2}$). Phototoxicity was also examined in A549, MCF-7 and CHO cell lines. IC_{50} values in the nanomolar range were obtained. Colony forming and cell proliferation assays revealed that complex **35** could relevantly reduce the colony growth of OCI-AML3 (myeloid leukemia cell line) (44% and 84.4%) and leukemic AE9a cell line (37% and 88%) when treated and irradiated for 2 min or 5 min, respectively. The conjugate reduced the healthy murine BM cells growth only by 10% and 28% upon light irradiation, clearly showing the specificity of the conjugate towards cancer cells. Since two photon absorbing PS offer deeper tissue penetration and better spatial resolution,[48] researchers

also looked at the TP properties of complex. Data obtained for **35** showed 5 times higher TP cross-section values for the conjugate than for the Ru(II) complex alone. This nanotransporter platform with enhanced cellular uptake, phototoxicity and specificity against a leukemic cell line is undoubtedly a successful solution for selective delivery of PDT PSs.

In 2018, a biological evaluation of the use of a Ru(II) complex conjugated with tamoxifen as a TP-PDT PS was published (see Figure 21 for structure).[49]The Estrogen Receptor (ER) is highly overexpressed in breast cancer cells, making it a great target for anticancer therapy.[50] For over 30 years, tamoxifen has been an approved drug for the endocrine treatment of oestrogen-receptor-positive breast cancer.[51]

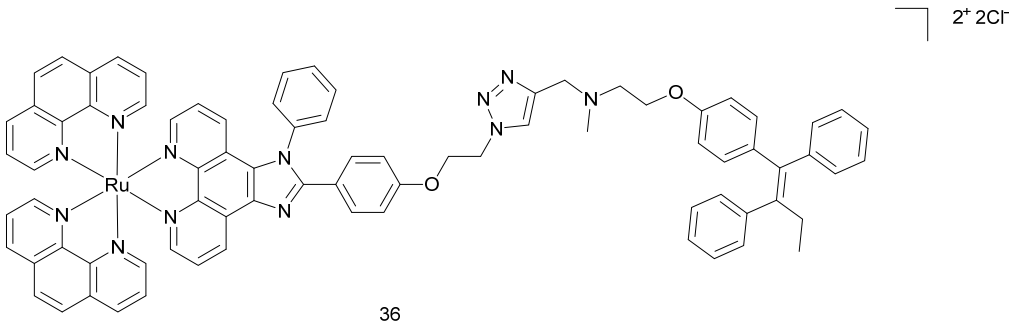

36

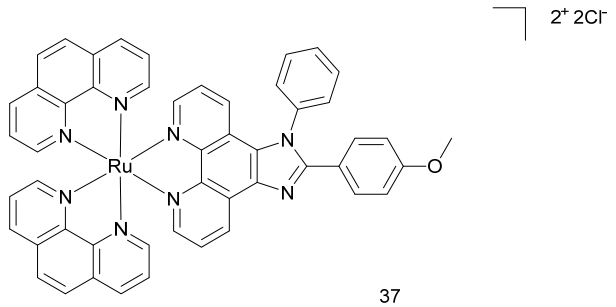

37

Figure 21. Chemical structure of complex **36** and **37**

The designed complex **36** demonstrated a large two-photon action cross section. The selectivity of complex **36** against cells overexpressing ER was confirmed by confocal microscopy in MCF-7 (ER positive), MDA-MB 231(ER negative) breast cancer cell lines as well as in HL-7702 (human liver) and COS-7 (monkey kidney) non-cancerous cell lines. Competitive assay with

17ϐ-estradiol (inhibitor of ER) showed that the uptake of complex **36** depended on interaction with the ER. Complex **36** as found to be non-toxic to cells in the dark. Upon light irradiation (450 nm, 12 $J \cdot cm^{-2}$) almost all MCF-7 cells treated with 16 μM of complex **36** were killed (99%) in comparison to the control (complex **37** which is not conjugated to tamoxifen, Figure 21). Calcein AM and PI staining confirmed these cytotoxicity studies. Annexin V and PI assays showed that the treated and irradiated cells were in late apoptosis or necrosis. ROS generation of the complex **36** was verified by DCFH-DA. Moreover, upon addition of NaN_3 (singlet oxygen scavenger), only very week fluorescence of the DCFH-DA was observed. Confocal microscopy studies showed that complex **36** localised in the lysosomes. Acridine orange (AO) staining demonstrated that upon light irradiation complex **36** caused lysosomes disruption. Very importantly, as a further confirmation of the mode of cell death action, complex **36** was found to generate singlet oxygen upon two-photon irradiation (fs, 820 nm) leading to cell death (calcein AM and PI staining).

Nanomaterials like carbon nanotubes or nanodots can also be used as carriers for different therapeutic drugs or diagnostic molecules.[52] In 2015, Zhang *et al*. developed carbon nanotubes functionalised with TP-absorbing Ru(II) complexes for bimodal photothermal and photodynamic therapy.[53] Two years later, a full biological evaluation of carbon nanodots modified with ruthenium complex was published.[54] This study showed that the combination with Ru(II) polypyridyl complexes might improve their intercellular uptake as well as their features required for PDT. For the studies, two complexes were used: complex **38** alone and complex **38** conjugated to carbon nanodots (see Figure 22 for structure of Ru(II) complex). These compounds exhibited TP phosphorescence as well as higher $^1O_2$ production in acidic environment than at neutral pH. Both compounds were taken up by A549 cells as well as normal LO2 cells, as confirmed by ICP-MS. The ruthenium content was estimated to be 10.6 ± 0.3 ng/10^6 cells for complex **38** and 16.2 ± 0.4 ng/10^6 for complex **38** with CDs in A549 cells and

6.0 ±0.2 ng/10^6 and 6.4 ±0.2 ng/10^6 in LO2 cells, indicating that CDs might improve the uptake into the cancerous cells.

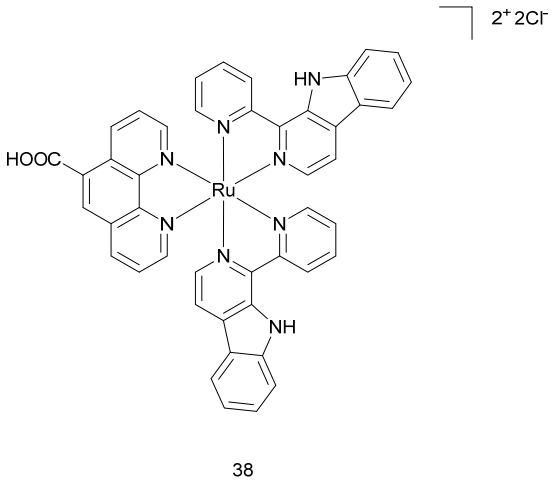

38

Figure 22. Chemical structure of complex **38**.

Cellular localisation performed by confocal laser microscopy showed that both compounds localised in the cytoplasm, specifically in the lysosomes. The cytotoxicity in the dark and after light irradiation (5 min; 450 nm; 20 $mW \cdot cm^{-2}$) was determined by cell proliferation assay (MTT) in A549 and LO2 cell lines. Complex **38** and complex **38** with CDs displayed high PI values (7.8 and 20.0 respectively) for the cancerous cell line compared to normal LO2 cells (>2.5 and 6.2). Complex **38** with CDs showed better results than the Ru (II) polypyridyl complex alone. To assess the type of mechanism causing cell death, the researchers performed multiple experiments. Cell morphology, annexin V staining, protein levels of caspase 3 and 7 as well as ATP levels in irradiated A549 cells confirmed that apoptosis was the main cause of cell death. This mechanism was likely triggered by the high amounts of $^1O_2$ produced in lysosomes, which caused lysosomal permeability. This hypothesis was further confirmed with confocal microscopy and flow cytometry analysis. To further investigate if complex **38** and complex **38** with CDs would be efficacious in solid tumours, the researchers performed several experiments on MCTSs. Complex **38** and complex **38** with CDs were found to be able to penetrate 400 µm

A549 spheroids. Confocal microscopy studies with calcein AM staining corroborated that spheroids treated with the compounds in the dark condition were viable and that cell death was only limited to the irradiated area. Once again, complex **38** with CDs was found to be better than ruthenium complex alone. IC_{50} values that were obtained on spheroids upon light irradiation (20 min; 810 nm; 100 mW; 80 mHz; 100 fs) were 12.0 µM for complex **38** (PI >8.3) and 2.2 µM for complex **38** with CDs (PI >45.5). Both compounds were successfully used as imaging agents in a living organism, namely zebrafish.

The PDT therapeutic potential of a PS is usually dependent on the oxygen levels in the targeted tissue since most of the PSs act with type II mechanism. In 2017, an interesting work on cyclometalated Ru(II) complexes, which act as Type I PSs, was published by Huang and co-workers.[55] The aim of this study was to design new PSs that could exhibit good PDT effects under hypoxia conditions. One of the designed PS contains a coumarin moiety (complex **39**) while the other one does not (complex **40**) (see Figure 23 for structures).

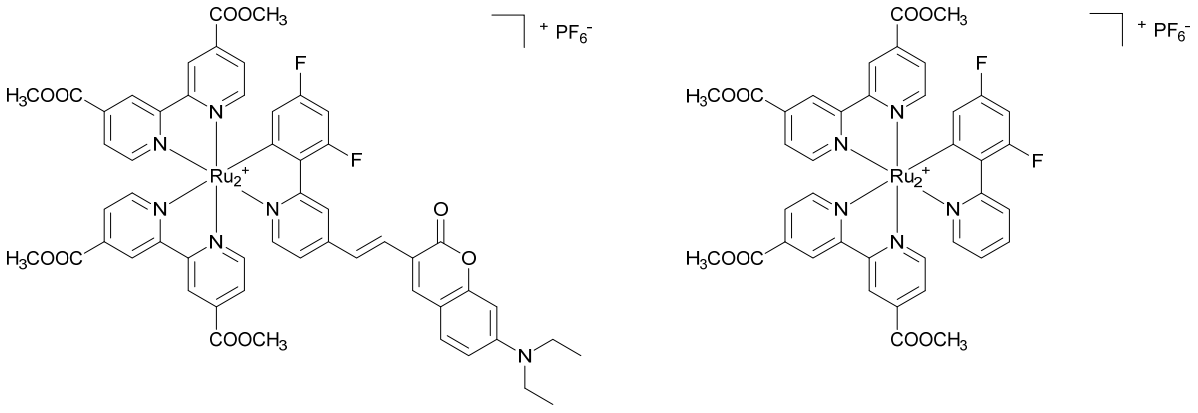

Figure 23. Chemical structure of complex **39** and complex **40**.

Coumarins have electron-donating and light-harvesting abilities. In both normoxia and hypoxia conditions, complex **39** showed low dark cytotoxicity and caused fast cell apoptosis after light irradiation in HeLa cells (white light; 400-800 nm, 30 mW cm^{-2}, 10 min). Cell death was confirmed with flow cytometry and fluorescent microscopy experiments. ROS generation

studies confirmed that complex **39** generated high level of ROS under hypoxic and normoxic conditions compared to complex **39** and $Ru(byp)_3^{2+}$, which were used as a control. Highly-oxidative hydroxyl radicals were detected after light irradiation. Complex **40** was a far less effective PS compared to complex **39**. To further verify the effectiveness of complex **39**, *in vivo* studies (HeLa derived tumours in mice) were performed. Dosage of 5 mg kg^{-1} of the PS caused tumour growth inhibition and serious tumour cell damage after irradiation (xenon lamp, 250 mW cm^{-2}, 15 min) (Figure 24). No side-effects during 14 days of treatment were observed. Histopathology as well as clearing time studies confirmed that complex **39** was not toxic for organs and was not accumulating in the body.

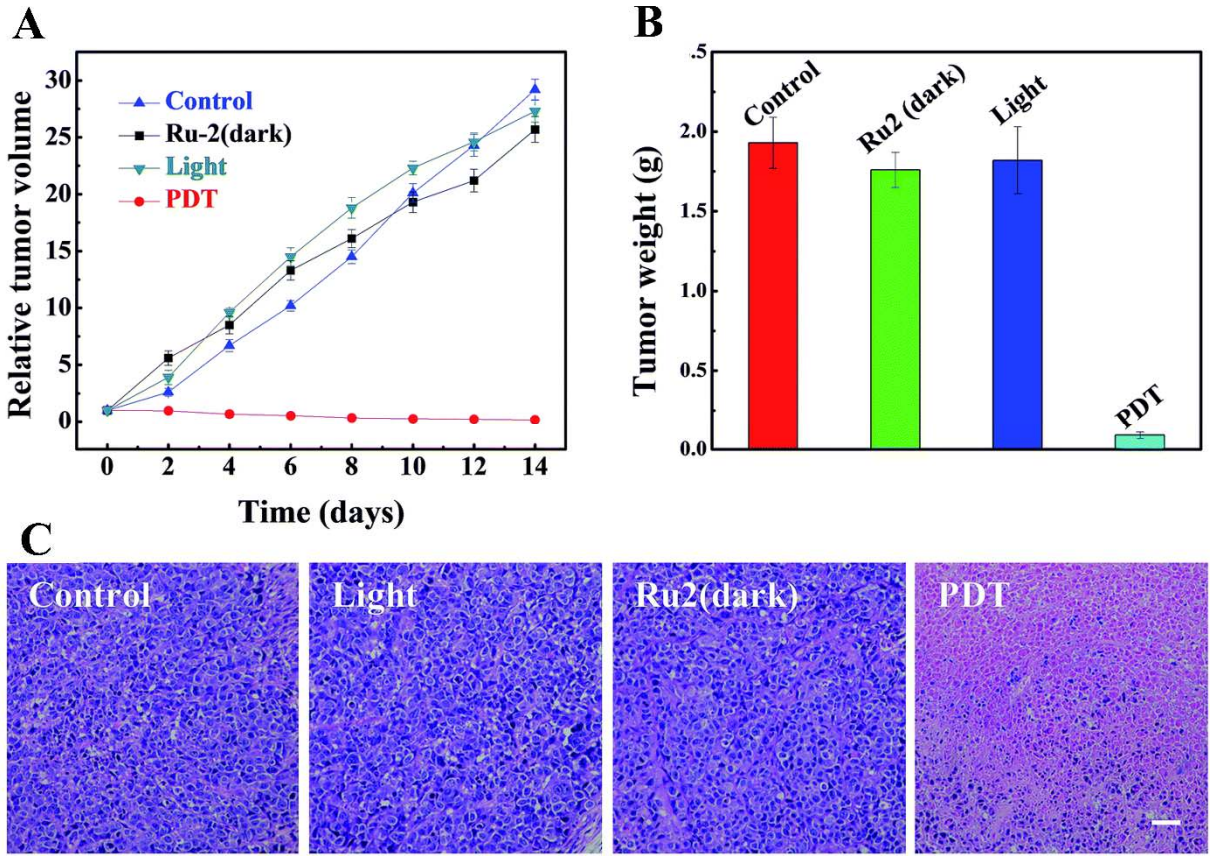

Figure 24.A. Relative tumor volume of different groups after various treatments.

B Tumor weights of different groups after 14 days treatments.

C. H&E stained tumor slices of different groups.

Figure taken from ref.56 with permission from The Royal Society of Chemistry

Complex **39** can be considered as a promising PS that can work under hypoxic conditions.

A recent study published by Keyes and co-workers introduced a Ru(II) complex conjugated with nuclear localisation signal (NLS). Such signal sequence was derived from nuclear factor –kappa B (NF-κB) (**41**, Figure 25),[56] a regulatory protein involved in the control of immune and inflammatory responses. Its activation is caused by different stimuli (e.g. growth factors, microbial components and stress agents)[57] and, mechanistically, requires nuclear translocation of the protein.

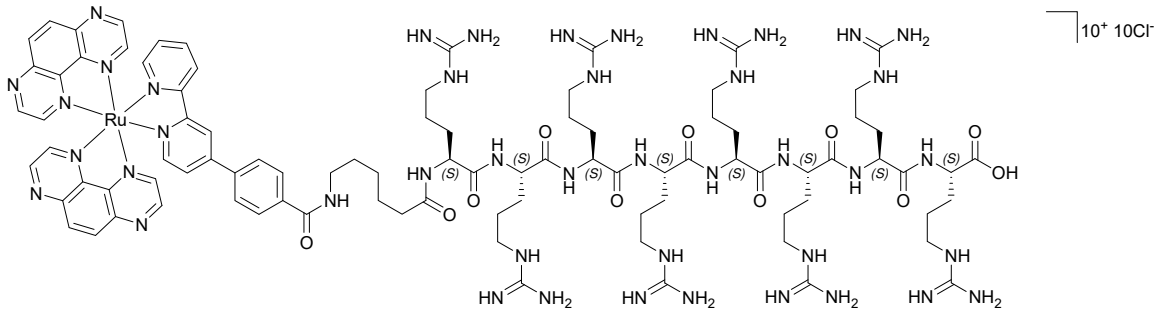

41

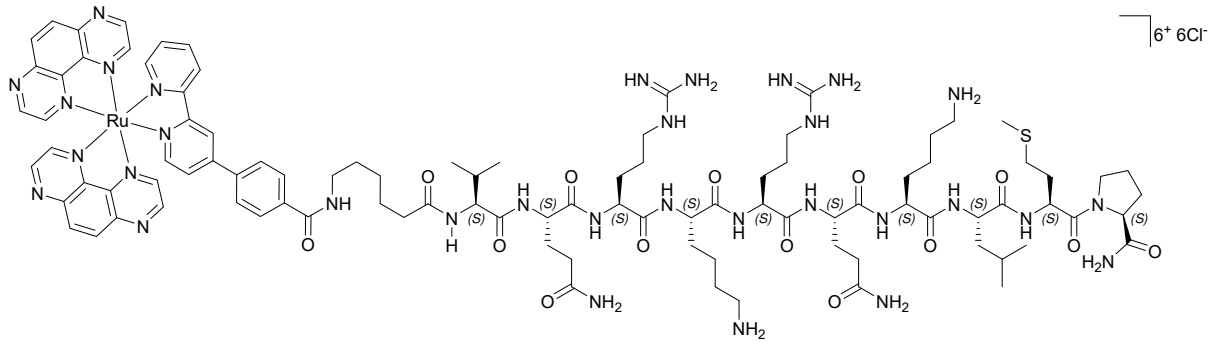

42

Figure 25. Chemical structure of complex **41** and complex **42**.

Complex **42** was found to localise in the cell nucleus of HeLa and CHO cell lines. On the contrary, complex **41** (Figure 18), which did not have a NLS but was conjugated with cell

permeable peptide, remained in the cell cytoplasm. Complex **42** was found to be taken up by cells through an energy-depended transport and to be not cytotoxic in the dark on HeLa cells (IC_{50} value of 83.4 μM). Light irradiation of treated cells at 440 nm (5 $mW \cdot cm^{-2}$, 15 min) lowered the IC_{50} value to 51.8 μM. Single cell irradiation experiments with cells treated with complex **42** or complex **41**, co-stained with nuclear dye DRAQ 7 (which only enters dead or permeabilised cells), demonstrated that the phototoxic effect of complex **42** was a result of its nuclear localisation. CT-DNA binding affinity studies along with photo-cleavage of pUC19 plasmid showed that complex **42** binds strongly DNA and is able to cleave it upon light irradiation. Tests with NaN_3 revealed that singlet oxygen was not responsible for DNA cleavage. It was proposed that either Type I mechanism of electron exchange or direct oxidative damage at the guanine bases was the cause of DNA damage.

Conclusions and outlook

In recent years, many Ru(II) polypyridyl complexes were studied as potential PDT PSs. Their strong absorption in the visible light, ability to produce singlet oxygen upon light irradiation, tunable photophysics and lack of cytotoxicity in the dark makes them very attractive candidates. Unfortunately, not many of them were analysed in-depth from a biological point of view. The mechanism of action of these compounds in living cells, a key factor in order to obtain their approval for a given indication, is very often still unknown or has only been superficially investigated. Worse, as shown in this Feature Article, there are only a few *in vivo* studies reported to date. However, despite this, one of such compounds has already entered clinical trial as a PDT PS against bladder cancer, clearly emphasising the potential of such complexes in this area of research. Further investigations in field of Ru(II) polypyridyl complexes as PDT PSs are of course needed. There is undoubtedly a necessity for new complexes that will exert their action by Type I mechanism. This is a crucial feature that will help fight very difficult to treat hypoxic tumours. During the designing process of the PDT PSs, adjustments will also need to be made in order to have PSs that can be activated at higher wavelengths. It is known that longer wavelengths will allow for deeper penetration through tissue. As shown in this Feature Article, this can also be obtained by Ru(II) polypyridyl complexes that are activated by two photon irradiation. However, this technique will require further proofs of its suitability for in vivo models, since studies in this field of research, not only with Ru(II) complexes, are for the moment much too scarce. Overall, we are convinced that this field of research is still in its infancy and that very exciting results will be published in the near future.

Abbreviations

5-ALA- aminolevulinic acid

AO- Acridine orange

CDs- carbon nanodots

CW- Continuus Wave lasers

DCFH-DA- 2,7-dichlorodihydro-fluorescein diacetate

DHE- dihydroethidium

Dppz- dipyridophenazine

EPR- Electron paramagnetic resonance

ER- Endoplasmic reticulum/ Estrogen Receptor

EthD-1- ethidium homodimer-

FACS- Fluorescent activated Cell Sorting

FLIM- Fluorescence Lifetime Imaging Microscopy

GSH- glutathione

HR-CS AAS- High-Resolution Continuum Source Atomic Absorption Spectrometry

HSA- Human Serum Albumin

IC_{50}- Inhibitory Concentration 50

ICP-MS- Inductively Coupled Plasma Mass Spectrometry

IP-TT- 2-(2',2'':5'',2'''-terthiophene)-imidazo[4,5-f][1,10]phenanthroline

ISC- Intersystem crossing

LD_{50}- Lethal Dose 50

MB- Methylene Blue

MCTS- Multicellular Tumour Spheroids

MMP – mitochondrial membrane potential

MTD_{50}- Maximum Tolerated Dose 50

MTT- cell proliferation assay

NAC- N-acetylcysteine

NADPH- Nicotinamide Adenine Dinucleotide Phosphate

NLS- nuclear localisation signal

OP- One-photon

PDI- Photodynamic inactivation

Pdppz- ([2,3-h]dipyrido[3,2-a:2’,3’-c]phenazine)

PDT- Photodynamic therapy

PI- Phototoxic index/ Propidium iodide

PLIM- Phospohorescence Lifetime Imaging Microscopy

PS- Photosensitiser

ROS- Reactive oxygen species

TP- Two photon

TPA- two photon absorption

TPP- Trisphenylphospine

TP-PDT- Two photon photodynamic therapy

Cell lines metioned

A549- pulmonary carcinoma

A549R- Cisplatin resistant ell line

AE9a- leukemia

BM- normal murine cells

CCD-1064sk- normal skin fibroblasts

CHO-K1/Ga- Chinese hamster ovarian epithelial cell line expressing Gα15 alpha subunit protein

CHO-K1/Ga15/SSTR2- Chinese hamster ovarian epithelial cell line expressing Gα15 alpha subunit protein and overexpressing somatostatin receptor 2

COS-7- monkey kidney cells

CRL5915- mesothelioma cell line

CT-26- wild type mouse colon carcinoma

CT-5.26- N-nitroso-N-methylurethane-induces mouse colon carcinoma

DG-75- Burkitt lymphoma

F98- rat glioblastoma

HCT116- colon cancer

HeLa- cervical cancer

HL-60- acute myeloid leuke

HL-7702- human normal liver cells

HT1367- urothelial cell line

KV- multi-resistant human oral floor carcinoma

LO2- human fetal hepatocyte

MCF-7- mammary gland adenocarcinoma

MDA-MB 231- ER negative breast cancer

MRC-5- normal lung fibroblast

Mutu-1- Epstein-Barr virus-related Burkitt lymphoma

OCI-AML3- myeloid leukemia

One58- mesothelioma cell line

PC-3- prostate cancer

RPE-1 retina pigmented epithelium

SK-MEL-28- melanoma cell line

T24- urothelial cell line

U2OS- human bone osteosarcoma

U87 MG- human glioblastoma

Biographies

Marta Jakubaszek graduated from Wrocław University of Science and Technology (Poland) with a Master of Engineering degree in 2014. During her studies, Marta took part in a Visiting Research Graduate Traineeship Program at University of Virginia (USA) working with HOPS complex and SNARE proteins. After graduation, Marta joined the laboratory of Dan Foltz at Northwestern University (USA) to work with Ruvbl1 and Ruvbl2 proteins and the assembly of centromeric chromatin. With a strong interest of learning more on chemical biology, Marta joined the Gasser group at Chimie ParisTech, PSL University (France) as a PhD student in 2017.

Bruno Goud is a Director of Research at the CNRS and chairman of the Cell Biology Department of the Institute Curie in Paris. His team is considered as a leading laboratory in the field of membrane trafficking. He co-authored over 200 publications. He is regularly invited to speak at international meetings and has organized several of them himself. He has coordinated and participated in several HFSP (Human Frontier Science Program) and European programs. He received an ERC (European Research Council) advanced grant in 2014. He was elected a member of EMBO in 2003. He belongs to the editorial board of several peer-reviewed international journals.

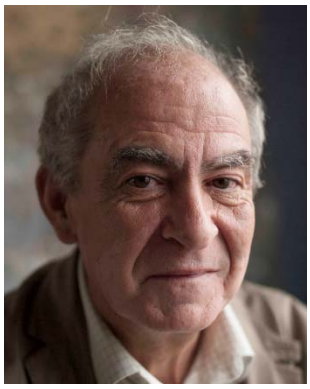

Stefano Ferrari performed his studies in Padua, Italy, and Dundee, Scotland, obtaining a PhD in Biochemistry. He then undertook post-doc with Prof. George Thomas at the Friedrich Miescher Institute, where he conducted studies leading to the identification of the mTOR-p70S6K pathway. Stefano was then Junior Group Leader at the Institute of Experimental Cancer Research at the University of Freiburg, Germany. After a brief stage at Novartis Pharmaceutical in Basel, he then moved to the Institute of Molecular Cancer Research at the University of Zurich, Switzerland, where he investigates issues related to DNA damage and the control of cell cycle transitions.

Gilles Gasser undertook a PhD thesis with Helen Stoeckli-Evans (University of Neuchâtel, Switzerland) and two post-docs with the late Leone Spiccia (Monash University, Australia) and Nils Metzler-Nolte (Ruhr-University Bochum, Germany). Gilles was then a Swiss National Science Foundation (SNSF) Ambizione Research Fellow and then an SNSF Assistant Professor at the University of Zurich (Switzerland). In 2016, Gilles moved to Chimie ParisTech, PSL

University (France). Gilles was the recipient of several awards including the Alfred Werner Award from the Swiss Chemical Society, an ERC Consolidator Grant, the Thieme Chemistry Journal Award and the Jucker Award for his contribution to cancer research.

Conflicts of interest

There are no conflicts to declare

Acknowledgments

This work was financially supported by an ERC Consolidator Grant PhotoMedMet to G.G. (GA 681679) and has received support under the program *Investissements d'Aveni*r launched by the French Government and implemented by the ANR with the reference ANR-10-IDEX-0001-02 PSL (G.G.) and by grants from the Stiftung zur Krebsbekämpfung and the Stiftung für wissenschaftliche Forschung of the University of Zurich (S.F.) and by grants from the Institut Curie and the Centre National de la Recherche Scientifique (CNRS) (B.G.).

References

1. D. Kessel, *Photodiag. Photodyn. Ther.*, 2004, **1**, 3-7.
2. X. Wen, Y. Li and M. R. Hamblin, *Photodiagn. Photodyn. Ther.*, 2017, **19**, 140-152.
3. S. Bonnet, *Dalton Trans.*, 2018, DOI: 10.1039/C8DT01585F.
4. J. Liu, C. Jin, B. Yuan, Y. Chen, X. Liu, L. Ji and H. Chao, *Chem. Comm.*, 2017, **53**, 9878-9881.
5. N. Malatesti, I. Munitic and I. Jurak, *Biophys. Rev.*, 2017, **9**, 149-168.
6. C. Mari, V. Pierroz, S. Ferrari and G. Gasser, *Chem. Sci.*, 2015, **6**, 2660-2686.
7. A. P. Castano, T. N. Demidova and M. R. Hamblin, *Photodiagn. Photodyn. Ther.*, 2004, **1**, 279-293.
8. J. Moan and K. Berg, *Photochem. Photobiol.*, 1991, **53**, 549-553.
9. P. Agostinis, K. Berg, K. A. Cengel, T. H. Foster, A. W. Girotti, S. O. Gollnick, S. M. Hahn, M. R. Hamblin, A. Juzeniene, D. Kessel, M. Korbelik, J. Moan, P. Mroz, D. Nowis, J. Piette, B. C. Wilson and J. Golab, *CA Cancer J. Clin.,* 2011, **61**, 250-281.
10. I. Yoon, J. Z. Li and Y. K. Shim, *Clin. Endosc.*, 2013, **46**, 7-23.
11. M. Triesscheijn, P. Baas, J. H. Schellens and F. A. Stewart, O*ncologist*, 2006, **11**, 1034-1044.
12. L. Zeng, P. Gupta, Y. Chen, E. Wang, L. Ji, H. Chao and Z.-S. Chen, *Chem. Soc. Rev.*, 2017, **46**, 5771-5804.
13. C. Mari and G. Gasser, *Chimia*, 2015, **69**, 176-181.
14. L. K. McKenzie, H. E. Bryant and J. A. Weinstein, *Coord. Chem. Rev.*, 2018, DOI: 10.1016/j.ccr.2018.03.020.
15. X. Li, A. K. Gorle, M. K. Sundaraneedi, F. R. Keene and J. G. Collins, *Coord. Chem. Rev.*, 2017, DOI: 10.1016/j.ccr.2017.11.011.
16. S. M. Cloonan, R. B. Elmes, M. Erby, S. A. Bright, F. E. Poynton, D. E. Nolan, S. J. Quinn, T. Gunnlaugsson and D. C. Williams, *J Med Chem*, 2015, **58**, 4494-4505.
17. Y. Arenas, S. Monro, G. Shi, A. Mandel, S. McFarland and L. Lilge, *Photodiagn. Photodyn. Ther.*, 2013, **10**, 615-625.
18. J. Fong, K. Kasimova, Y. Arenas, P. Kaspler, S. Lazic, A. Mandel and L. Lilge, *Photochem. Photobiol. Sci.*, 2015, **14**, 2014-2023.
19. O. Dömötör, C. G. Hartinger, A. K. Bytzek, T. Kiss, B. K. Keppler and E. A. Enyedy, *JBIC J. Biol. Inorg. Chem.*, 2013, **18**, 9-17.
20. A. Levina, A. Mitra and P. A. Lay, *Metallomics*, 2009, **1**, 458-470.
21. S. Tortorella and T. C. Karagiannis, *J. Membr. Biol.*, 2014, **247**, 291-307.
22. S. V. Torti and F. M. Torti, Crit. Rev. Oncog., 2013, **18**, 435-448.
23. P. Kaspler, S. Lazic, S. Forward, Y. Arenas, A. Mandel and L. Lilge, *Photochem. Photobiol. Sci.*, 2016, **15**, 481-495.
24. S. Kalinina, J. Breymayer, K. Reess, L. Lilge, A. Mandel and A. Ruck, *J. Biophotonics*, 2018, DOI: 10.1002/jbio.201800085, e201800085.
25. G. Ghosh, K. L. Colón, A. Fuller, T. Sainuddin, E. Bradner, J. McCain, S. M. A. Monro, H. Yin, M. W. Hetu, C. G. Cameron and S. A. McFarland, *Inorg. Chem.*, 2018, **57**, 7694-7712.
26. Y.-L. P. Ow, D. R. Green, Z. Hao and T. W. Mak, *Nat. Rev. Mol. Cell Biol.*, 2008, **9**, 532.
27. V. Ramu, S. Aute, N. Taye, R. Guha, M. G. Walker, D. Mogare, A. Parulekar, J. A. Thomas, S. Chattopadhyay and A. Das, *Dalton Trans*, 2017, **46**, 6634-6644.
28. J. Hess, H. Huang, A. Kaiser, V. Pierroz, O. Blacque, H. Chao and G. Gasser, *Chem. - Eur.J.*, 2017, **23**, 9888-9896.
29. J. Liu, Y. Chen, G. Li, P. Zhang, C. Jin, L. Zeng, L. Ji and H. Chao, *Biomaterials*, 2015, **56**, 140-153.
30. C. W. T. Leung, Y. Hong, S. Chen, E. Zhao, J. W. Y. Lam and B. Z. Tang, *J. Am. Chem. Soc.*, 2013, **135**, 62-65.
31. L. Zeng, S. Kuang, G. Li, C. Jin, L. Ji and H. Chao, *Chem. Comm.*, 2017, **53**, 1977-1980.
32. Z. Zhou, J. Liu, T. W. Rees, H. Wang, X. Li, H. Chao and P. J. Stang, *Proc. Nat. Acad. Sci.U.S.A.*, 2018, **115**, 5664-5669.

33. A. M. Angeles-Boza, P. M. Bradley, P. K. Fu, S. E. Wicke, J. Bacsa, K. R. Dunbar and C. Turro, *Inorg. Chem.*, 2004, **43**, 8510-8519.
34. A. J. McConnell, H. Song and J. K. Barton, *Inorg. Chem.*, 2013, **52**, 10131-10136.
35. C. Mari, V. Pierroz, R. Rubbiani, M. Patra, J. Hess, B. Spingler, L. Oehninger, J. Schur, I. Ott, L. Salassa, S. Ferrari and G. Gasser, *Chem. Eur. J.,* 2014, **20**, 14421-14436.
36. A. E. Friedman, J. C. Chambron, J. P. Sauvage, N. J. Turro and J. K. Barton, *J. Am. Chem. Soc.*, 1990, **112**, 4960-4962.
37. V. Pierroz, R. Rubbiani, C. Gentili, M. Patra, C. Mari, G. Gasser and S. Ferrari, *Chem Sci*, 2016, **7**, 6115-6124.
38. A. J. McConnell, M. H. Lim, E. D. Olmon, H. Song, E. E. Dervan and J. K. Barton, *Inorg. Chem.*, 2012, **51**, 12511-12520.
39. M. Dickerson, Y. Sun, B. Howerton and E. C. Glazer, *Inorg Chem*, 2014, **53**, 10370-10377.
40. C. Mari, R. Rubbiani and G. Gasser, *Inorg. Chim. Acta*, 2017, **454**, 21-26.
41. H. Huang, B. Yu, P. Zhang, J. Huang, Y. Chen, G. Gasser, L. Ji and H. Chao, *Angew. Chem., Int. Ed. Engl.*, 2015, **54**, 14049-14052.
42. G. L. Zwicke, G. A. Mansoori and C. J. Jeffery, *Nano Rev.*, 2012, **3**.
43. C. M. A. Alonso, A. Palumbo, A. J. Bullous, F. Pretto, D. Neri and R. W. Boyle, *Bioconjugate Chem.*, 2010, **21**, 302-313.
44. T. Wang, N. Zabarska, Y. Wu, M. Lamla, S. Fischer, K. Monczak, D. Y. W. Ng, S. Rau and T. Weil, *Chem. Comm.*, 2015, **51**, 12552-12555.
45. P. Rorsman and M. O. Huising, *Nat. Rev. Endocrinol.*, 2018, DOI: 10.1038/s41574-018-0020-6.
46. L. C. Sun and D. H. Coy, *Curr. Drug Deliv.*, 2011, **8**, 2-10.
47. S. Chakrabortty, B. K. Agrawalla, A. Stumper, N. M. Vegi, S. Fischer, C. Reichardt, M. Kogler, B. Dietzek, M. Feuring-Buske, C. Buske, S. Rau and T. Weil, *J. Am. Chem. Soc.*, 2017, **139**, 2512-2519.
48. G. B. Magali, M. Youssef, R. Cédric, B. David, B. Ilaria, M. Marie, V. Ophélie, M. Olivier, B. D. Mireille, M. Alain, G. Marcel, D. Jean-Olivier and R. Laurence, *Angew. Chem., Int. Ed. Engl.*, 2011, **123**, 11627-11631.
49. X. Zhao, M. Li, W. Sun, J. Fan, J. Du and X. Peng, *Chem. Comm.*, 2018, **54**, 7038-7041.
50. S. I. Hayashi, H. Eguchi, K. Tanimoto, T. Yoshida, Y. Omoto, A. Inoue, N. Yoshida and Y. Yamaguchi, *Endocr. Relat. Cancer*, 2003, **10**, 193-202.
51. V. C. Jordan, *Nat. Rev. Drug Discov.*, 2003, **2**, 205.
52. L. Muzi, C. Menard-Moyon, J. Russier, J. Li, C. F. Chin, W. H. Ang, G. Pastorin, G. Risuleo and A. Bianco, *Nanoscale*, 2015, **7**, 5383-5394.
53. P. Zhang, H. Huang, J. Huang, H. Chen, J. Wang, K. Qiu, D. Zhao, L. Ji and H. Chao, *ACS Appl. Mater. Inter.*, 2015, **7**, 23278-23290.
54. D. Y. Zhang, Y. Zheng, H. Zhang, L. He, C. P. Tan, J. H. Sun, W. Zhang, X. Peng, Q. Zhan, L. N. Ji and Z. W. Mao, *Nanoscale*, 2017, DOI: 10.1039/c7nr05349e.
55. Z. Lv, H. Wei, Q. Li, X. Su, S.-J. Liu, K. Y. Zhang, W. Lv, Q. Zhao, X. Li and W. Huang, *Chem. Sci.*, 2017, DOI: 10.1039/C7SC03765A.
56. C. S. Burke, A. Byrne and T. E. Keyes, *J. Am. Chem. Soc.*, 2018, DOI: 10.1021/jacs.8b02711.
57. T. Liu, L. Zhang, D. Joo and S.-C. Sun, *Signal Transduction And Targeted Ther.*, 2017, **2**, 17023.